THESIS

LASING AT 52.9 NM IN NE-LIKE CHLORINE AND STEPS TOWARDS SHORTER WAVELENGTH CAPILLARY DISCHARGE LASERS

Submitted by

Maximo Frati

Department of Electrical and Computing Engineering

In partial fulfillment of the requirements

for the Degree of Master of Science

Colorado State University

Fort Collins, Colorado

Spring 2001

COLORADO STATE UNIVERSITY

March 23, 2001

WE HEREBY RECOMMEND THAT THE THESIS PREPARED UNDER OUR SUPERVISION BY MAXIMO FRATI ENTITLED LASING AT 52.9 NM IN NE-LIKE CHLORINE AND STEPS TOWARDS SHORTER WAVELENGTH CAPILLARY DISCHARGE LASERS BE ACCEPTED AS FULFILLING IN PART REQUIREMENTS FOR THE DEGREE OF MASTER OF SCIENCE.

Committee on graduate work

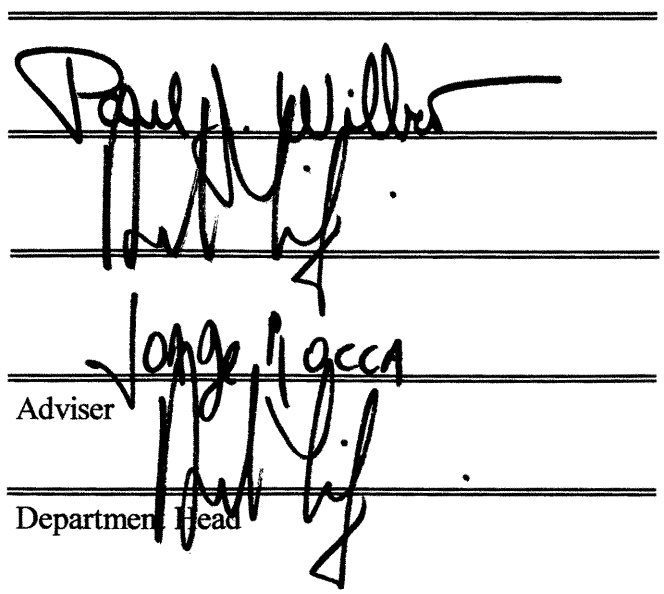

Adviser

Department Head

ABSTRACT OF THESIS

LASING AT 52.9 NM IN NE-LIKE CHLORINE AND STEPS TOWARDS SHORTER WAVELENGTH CAPILLARY DISCHARGE LASERS

Significant advances have been obtained in the past few years in the development of soft x-ray lasers. Both, laser-pumped and discharge-pumped schemes have been successfully demonstrated. In particular, a very compact capillary discharge laser has been demonstrated to deliver an average power of several mW in the 46.9nm line of Ne-like Ar.

The work presented in this thesis, that was motivated by the possibility extending the very practical discharge excitation scheme to other short wavelengths laser transitions, can be divided in two parts. The first resulted in the successful demonstration of amplified spontaneous emission in the $3p\,^1S_0$-$3s\,^1P_1$ transition of Ne-like Cl at 52.9 nm. Laser pulses of ~1.5 ns duration with energies up to 10 μJ and a beam divergence 4 mrad were obtained at repetition rates of 0.5 – 1 Hz. This new 23.4 eV table top laser is of particular interest for applications requiring high peak fluxes of photons with energy

slightly below the He photoionization threshold. The results discussed in the second part of this thesis represent the first steps necessary for the development of a discharge–pumped Ni-like Cd laser at 13.2 nm. A room temperature source of atomically pure Cd vapor was developed and used to inject Cd into the capillary channel, where it was excited by a fast high current pulse to produce a hot dense plasma. The first spectroscopic data of a capillary discharge plasma containing Ni-like Cd ions (Cd_{XXI}) was obtained and analyzed. These results can be of use in future works when trying to develop a collisionally excited discharge-pumped Ni-like Cd laser.

Maximo Frati
Department of Electrical
and Computing Engineering
Colorado State University
Fort Collins, CO 80526
Spring 2001

To my wife Silvina.

TABLE OF CONTENTS

CHAPTER I

1.1. Introduction

Several motivations exist for the development of practical soft x-ray lasers. They include studies in atomic physics, photochemistry and photophysics, lithography, very high density plasmas diagnostics, also in the future, when the wavelength drops below 1 nm, x-ray lasers will allow time-resolved x-ray diffractometry of biological and inorganic substances and medical diagnostics.

Before focusing on the discussion of soft x-ray lasers, it should be mentioned that the direct amplification of radiation in plasmas is not the only mean by which coherent soft x-ray radiation can be generated. Other techniques include synchrotron sources[1-3], free electron lasers (FEL)[4], and harmonic up-conversion of high power optical lasers[5-7]. Synchrotron sources have the great advantages of broad tunability and high average power. However, they have low peak brightness, and are very large and expensive to build. Self-amplified soft x-ray emissions in FEL lasers are expected to have better coherence and radiate at higher power than synchrotron sources, but still they are in their infancy and far from being table-top devices. For a high order harmonic pulse, the highest

energy reported using a powerful glass laser was 60 nJ at a photon energy of about 50 eV, which corresponds $7.5 \cdot 10^9$ photons per pulse[7].

Although all the systems previously mentioned produce coherent soft x-ray radiation, their size, cost or average power, requires improvement to allow their widespread use in the applications mentioned above. Therefore, the development of more accessible schemes for the generation of soft x-ray lasers becomes important. One very convenient approach is the discharge pumping scheme which was proved to be successful in 1994 when large amplification was first obtained at 46.9 nm in Ne-like Ar. A very compact system developed based on this approach is capable of generating laser pulses with an average energy of 0.88 mJ at 4 Hz repetition rate corresponding to an average power of 3.5 mW. At an energy per photon of 26.5 eV, this flux corresponds to $2 \cdot 10^{14}$ photons per pulse[8]. Lasing by discharge excitation was also demonstrated in Ne-like S at 60.8 nm[93].

The objective of this thesis is the development of methods necessary to extend capillary discharge pumped lasers to other wavelengths. The work completed as part of this thesis can be divided in two parts. The first part, discussed in Chapter II, consists in the demonstration of lasing at 52.9 nm in Ne-like Chlorine[9]. Laser output pulses with an energy up to 10 uJ were obtained in this line, at a repetition rate of 0.5 Hz by modifying existing hardware that was previously used to obtain lasing at 46.9nm in Ne-like Argon. The laser beam characteristics were studied, yielding a divergence of approximately 4 mrad. Chapter III discusses the second part of the research, in which the first results of capillary discharge created metal vapor plasmas are presented as an approach to the development of shorter wavelength soft x-ray lasers. For this purpose a new method for

creating cadmium vapor at room temperature was developed. Spectra corresponding to cadmium up to twenty times ionized are analyzed for different discharge parameters with the purpose of characterizing the plasma behavior. The results are useful as a step toward optimizing the plasma condition for lasing.

The rest of this chapter discusses the collisional electron excitation scheme used in our experiments and summarizes the pumping techniques that have been developed to realize collisional soft x-ray lasers.

1.2. Collisional electron excitation

The electron impact excitation was one of the first soft x-ray laser schemes investigated theoretically in detail[10-15]. Collisional electron impact excitation of Ne-like and Ni-like ions has resulted in some the most robust soft x-ray lasers available. In the traditional implementation of these lasers the generation of a population inversion occurs in a quasi-cw regime by strong collisional monopole electron excitation of the laser upper level, aided by the very favorable ratio between the radiative lifetime of the laser upper and lower levels. The upper levels are metastable with respect to radiative decay to the ground state, and the laser lower levels are depopulated by strong dipole-allowed transitions.

The first successful demonstration of lasing at soft x-ray wavelengths utilizing this approach, realized at Lawrence Livermore National Laboratory, involved the $2p^5\,3p - 2p^5\,3s$ transitions in Ne-like Se and Ne-like Y[16].

While any $2p^n$ ($n=1$ to 6) isoelectronic sequence can be used in principle[17], the $n=6$ Ne-like sequence[18] has proven to be the most successful configuration in this type of system. This is at least partially due to the greater stability of this ions in a transient plasma, which is associated with the higher ionization potential of their closed shell configuration. Following the first successful results in Ne-like Se, lasing has been extended to nearly all of the Ne-like ions having atomic number between Si[19] and Ag[20] with wavelengths ranging from 87 nm to 9.93 nm. Figure 1.1 shows a simplified energy level diagram for a typical Ne-like system illustrating the laser transitions and the dominant processes involved in the generation of amplification. Also shown in this diagram is how this scheme extends with Ni-like ions. In this case the laser transitions take place between $n=4$ levels,such that $\Delta n=0$[21]. The 3p laser upper (4d for Ni-like) levels are dominantly populated by electron monopole collisional excitation from the ion ground state and by cascades from higher energy levels.

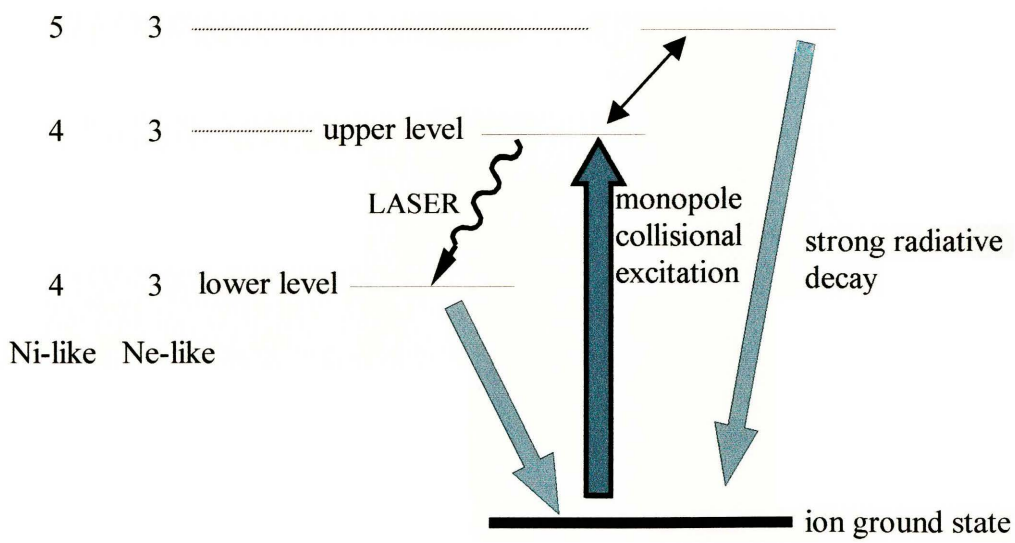

Figure 1.1. Energy level diagram for the Ne-like and Ni-like collisional laser schemes. In Ne-like lasers, the amplification occurs for transitions between 3p and 3s energy levels. In the Ni-like scheme the transitions amplified are the 4d-4p.

The population inversions are maintained by the very rapid radiative decay of the 3s laser lower levels (4p for Ni-like) to the ground state of the ion through strong dipole-allowed transitions. Therefore, operation of these lasers in a quasi-cw regime requires the plasma to be optically thin for the transitions originating from the laser lower level. Lasers in the $3d^9\,4d - 3d^9\,4p$ transitions of Ni-like ions are in direct analogy to $2p^5\,3p - 2p^5\,3s$ laser transitions in closed shell Ne-like ions, but have the advantage of producing amplification at shorter wavelength for a given state of ionization. This higher quantum efficiency for Ni-like ions significantly reduces the pumping energy required to achieve lasing at a selected wavelength. Ni-like soft x-ray lasers were first demonstrated in 1987 in an Eu laser-created plasma, producing a gain length product $gl \approx 4$ at 7.1 nm[22]. Subsequently, the scheme was isoelectronically extrapolated to other ions with laser wavelengths as short as 3.56 nm in Ni-like Au[23]. Recently, gain saturation has been obtained at wavelengths as short as 5.8 nm[24]. Gain has also been observed in Co-like ions[23], and the use of the Nd-like sequence has also been proposed[25].

Different pumping methods can be used to collisionally excite the soft x-ray laser transitions. Two very successful schemes, discussed next in this chapter, are the use of powerful optical lasers and fast capillary discharges.

1.2.1. Pumping using optical lasers

The collisionally excited soft x-ray lasers developed before 1990 consisted in laser created plasmas generated by focusing optical laser pulses into solid targets. The

energies of the pump laser pulses range from several hundred Joules to several kilo-Joules, and therefore involving the use of very large facilities[16,19,20,22,23,26-33]. The typical experimental set up used to generate one such laser is schematically illustrated below in figure 1.2.

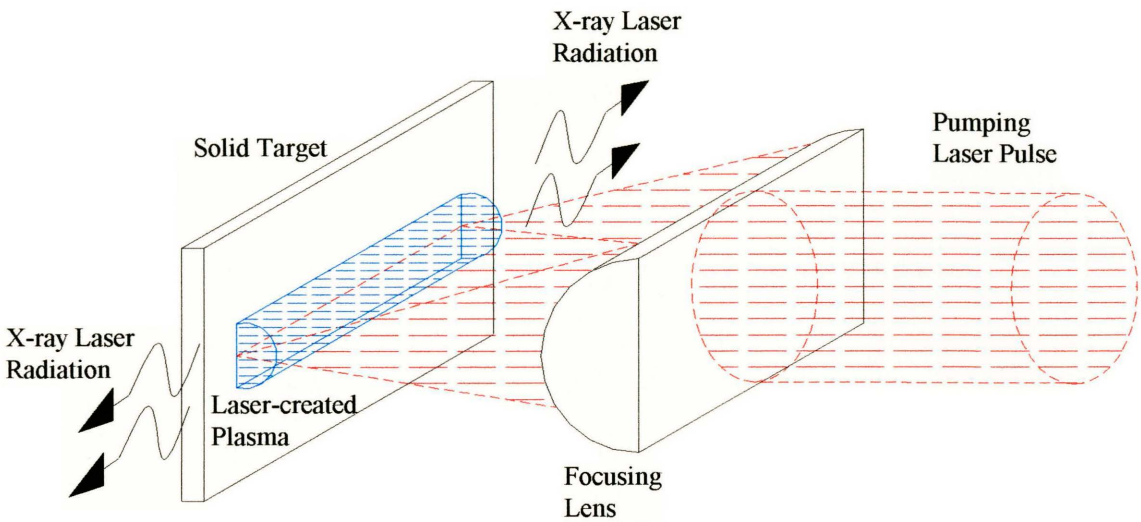

Figure 1.2. Scheme showing the generation of x-ray laser radiation using focused laser light as pumping scheme. A short laser pulse is line focused onto a solid target using a cylindrical lens. The laser pulse ablates material, creating and heating a high density plasma with the favorable conditions for lasing by collisional electron excitation.

In the last several years much progress has been made in improving the laser efficiency of collisional soft x-ray lasers. Strong refraction of the amplified laser beam, caused by the large electron density gradients in the amplifier, was recognized early as a major obstacle to the generation of efficient soft x-ray lasers with good beam quality. Some of the methods implemented to mitigate refraction are the use of foil targets[16,34], opposite-gradient targets and curved targets[35-38], and in particular the use of one or multiple pre-pulses[39-61]. In the pre-pulse technique the first pulse is used to create a

plasma with an optimized density for amplification and with reduced density gradients for improved beam propagation. The subsequent pulses, which are more efficiently absorbed in the gain region, heat the plasma to lasing conditions. This pumping method leads to the observation of large amplification in a large number of elements with dramatic increase in the J = 0-1 laser line intensity and reduced excitation energy. Another important step in the reduction of the pump laser energy has been the use of shorter excitation pulses. Daido et al. reported lasing in several lanthanide ions in the spectral region between 5.8 nm and 14 nm using a three-prepulse sequence and a main excitation pulse of 100 ps duration and 250 J of energy[62,63]. A subsequent series of experiments conducted at Rutherford Laboratories obtained gain saturation in several transitions[64-67] with wavelengths as short as 5.86 nm (Ni-like Dy[68]) using sequences of 75 ps duration pump pulses with about 100 J of energy. Balmer and co-workers used a relatively compact Nd:glass laser to demonstrate saturated lasing in Ne-like Fe (25.5 nm), Ni-like Ag (14.0 nm) and Ni-like Pd (14.7 nm) with driving energies below 30 J in a 100 ps pulse[59-61]. In terms of improving the soft x-ray output beam characteristics double pass amplification experiments have demonstrated increased spatial coherence and reduced beam divergence[94].

The collisional electron excitation scheme described above is intrinsically a quasi-steady state scheme in which lasing can occur for as long as the plasma conditions necessary for the generation of a population inversion are maintained. It was first recognized by Afanasiev and Shlyaptsev[69] that one to two orders of magnitude larger gain coefficients can be produced for a short period of time (typically sub-picosecond to tens of picoseconds) by heating the plasma faster than the relaxation rate of the excited

states. The larger gain coefficients are mainly the consequence of the larger rate of excitation of the laser upper level from the ion ground state by electron collisions, that results in a large population inversion before collisions have time to redistribute the populations. Another phenomenon that contributes to a larger gain is the increased rate of electron excitation in an overheated plasma. Transient gains greater than $100\ cm^{-1}$ have been predicted theoretically[69,70]. In the transient regime there is no need to limit the transverse dimension of the plasma in order to ensure optical transparency of the laser lower level radiation. A main advantage of the transient excitation scheme for the realization of table-top x-ray lasers is the greatly reduced laser pump energy required for excitation. The recent availability of multi-terawatt ultrashort pulse optical laser systems with output energies of several Joules opened the opportunity to demonstrate soft x-ray lasing by transient electron collisional excitation[71-77]. The implementation is based on a two-step excitation sequence. First, a long laser pulse (typically nanosecond duration) is used to produce a plasma containing the desired active ions, which again are usually closed shell Ne-like or Ni-like ions. The temperature of the plasma generated with this pre-pulse must be sufficiently high to produce an abundant ground state population of these ions, but does not need to reach the values necessary to populate the laser upper level. The plasma is allowed to expand hydrodynamically to reach the desired degree of ionization, optimum electron density, and minimum possible electron density gradient. Second, the plasma is heated with a picosecond or subpicosecond laser pulse to rapidly increase the electron temperature to values that exceed the excitation energy of the laser upper level. The ionization balance is not significantly altered and a large transient population inversion is generated by electron excitation. The first demonstration of

amplification by transient inversion was realized by Nickles et al. in the 32.6 nm line of Ne-like Ti[71]. The experiment used a hybrid CPA Ti-sapphire/Nd:glass pump laser delivering a long laser pulse of 1.2 ns duration and 3 J of energy, synchronized with a short laser pulse of 0.7 ps duration and 2 J of energy. The soft x-ray laser pulse duration was measured to be less than 20 ps. The results were analyzed to correspond to an average gain of 19 cm^{-1} and a gain-length product $gl \approx 9.5$ [71]. Weaker lasing was also observed in a line near 30 nm, identified as the $3d-3p$, J = 1-1 transition in Ne-like Ti. These results were improved and extended to other Ne-like ions (such as Fe and Ge) and Ni-like ions in subsequent experiments conducted at several laboratories[72-77]. Dunn et al. reported gains of up to 35 cm^{-1} and $gl \approx 12.5$ in the $4d\ ^1S_0 - 4p\ ^1P_1$ line in Ni-like Pd at 14.7 nm[72], and large amplification in several other Ni-like ion transitions. The gain coefficient for target lengths between 1 and 2 mm was about 35 cm^{-1}, but continuously decreased to reach a value of 3.9 cm^{-1} for target lengths above 7 mm. This smooth decrease of the gain with target length has been observed in all non-traveling wave transient collisional excitation experiments, and resembles gain saturation. However, it is mainly caused by the short duration of the gain and by refraction. Gain saturation with the transient excitation scheme was first demonstrated on the Ne-like scheme for the 32.6 nm line of Ne-like Ti and the 19.6 nm line of Ne-like Ge at Rutherford Laboratories[74]. However, these experiments utilized a total reported excitation energy of 32 J and 60 J respectively, which is not available in smaller facilities. To achieve gain saturation with smaller excitation energy, traveling wave excitation schemes have been implemented at several laboratories. The short gain duration in these transient systems, T_g, limits the amplification length to values less than cT_g (where c is the speed of light in the plasma),

unless traveling wave excitation is used to maintain the excitation in phase with the amplified x-ray pulse. A traveling wave system was used to demonstrate gain saturation in Ni-like Pd at 14.7 nm with 1.8 J of long pulse energy and 5.2 J of short pulse. With the traveling wave excitation scheme, an increase in x-ray laser intensity of 20 to 100 times was observed with respect to the no traveling wave configuration[75]. The soft x-ray laser output energy with traveling wave excitation was estimated to be approximately $10\,\mu J$. Strong amplification was also obtained in Ni-like ion ranging from Mo (18.9 nm) to Sn (11.9 nm)[75]. A different traveling wave method was also used at Rutherford to obtain gain saturation in several Ne-like ions and in Ni-like Sm at 7.3 nm[76]. Experiments conducted at CEA-Limeil yielded gain saturation in the 13.9 nm laser line of Ni-like Ag and also observed strong amplification at 16.05 nm in a $4f-4d$ transition in the same ion[77]. Future improvements in pumping efficiency resulting from optimized target configurations and traveling wave excitation can be expected to lead to saturated transient inversion soft x-ray lasers occupying a single optical table, and to tabletop lasers that operate at shorter wavelengths.

Another method for pumping collisional lasers in which traveling wave excitation is intrinsic was demonstrated by Lemoff et al. in Pd-like Xe utilizing optical field ionization[78]. In this scheme an intense circularly polarized femtosecond laser pulse is used to simultaneously create close shell ions and hot pumping electrons by tunneling ionization. In the experiment the excitation was provided by circularly polarized laser pulses with an energy of 70 mJ and a duration of 40 fs generated by a CPA Ti:sapphire laser operating at 10Hz. The radiation of the pump laser was longitudinally focused onto a Xe gas target to tunnel-ionize the atoms to the Pd-like stage and produce hot electrons

that collisionally excite the laser upper level. The pump laser was focused by a 50 cm focal length mirror to an intensity greater than $3 \cdot 10^{16} \frac{W}{cm^2}$. An amplification of $gl \approx 11$ was measured in the 41.8nm line of Pd-like Xe for a cell length of 8.4 mm. Subsequent experiments determined that to achieve a high gain it is critical to avoid a significant pre-pulse in the femtosecond pump pulse[95].

1.2.2. Fast capillary discharge pumped lasers

In 1994, six years after capillary discharges were proposed as pumping schemes for compact high efficiency soft x-ray lasers[79], the first observation of large soft x-ray amplification in a discharge created plasma was realized by Rocca et al. in the $3s\ ^1P_1^0 - 3p\ ^1S_0$ transition of Ne-like argon at 46.9 nm[80,81]. In that initial experiment, current pulses of 60 ns half-cycle duration and 40 kA peak amplitude were used to excite Ar plasma columns 4 mm in diameter and up to 12 cm in length. The capillary was placed in the axis of a 3 nF liquid dielectric capacitor as it is shown in figure 1.3, and was pulse-charged by a Marx generator The capillary loads were excited by discharging the capacitor through a spark-gap switch pressurized with SF_6. A small gain was also observed in the J=2-1 1ine of Ne-like Ar at 69.8 nm[81]. The optimum conditions for lasing occur several ns before stagnation, when the first compression shock wave reaches the axis. Lasing by collisional electron excitation of Ne-like Ar ions takes place at a time when the electron density is rapidly increasing and reaches a value of $0.3 - 1 \cdot 10^{19} cm^{-3}$,

and when the electron temperature is around 60-80 eV[82]. The laser pulsewidth is approximately 1 ns in duration[81,83]. Subsequent experiments employing longer plasma columns under better optimized discharge conditions yielded an effective gain-length product $gl \approx 27$ and resulted in the first observation of gain saturation in a table-top soft x-ray amplifier[82]. Saturation of the laser intensity was observed at gain-length products of about 14[82].

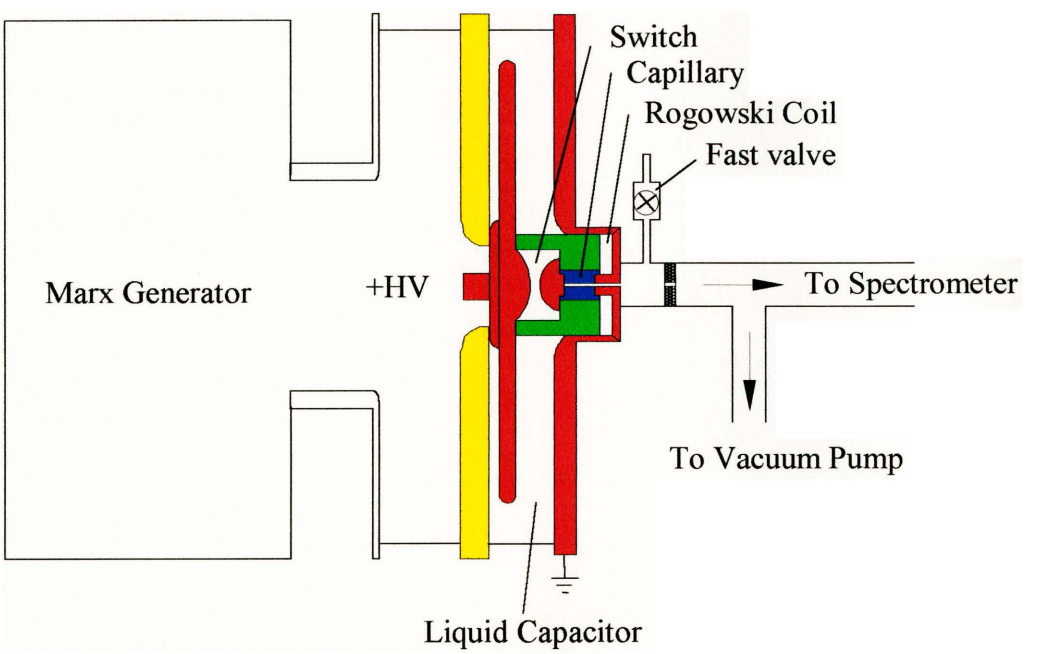

Figure 1.3. Schematic of the capillary discharge setup utilized by Rocca et al., to achieve coherent amplification in Ne-like Ar. A modified set up was used by Tomasel et al. to obtain lasing in Ne-like S[93].

In this type of discharge pumped amplifiers, the duration of the gain is usually shorter than the time required for the effective use of an optical cavity. Consequently,

discharge-pumped soft x-ray lasers operate without a cavity with a single pass amplification of the spontaneous emission. Then, the spectrally integrated intensity of the laser line depends on the length of the medium as:

$$I = \left(\frac{E}{g}\right)\left(e^{gl} - 1\right)^{3/2}\left(gle^{gl}\right)^{-1/2}$$

where g is the small signal gain coefficient, l is the length of the medium, and E is a constant proportional to the emissivity[84]. This exponential amplification continues until the saturation intensity value is reached. The circles in figure 1.4 represent experimental data for the intensity of the 46.9 nm laser transition in Ne-like Ar versus the length of the medium. The solid line corresponds to the fit of those values using the previous formula (Linford). From the fit, a value of $g = 0.92\ cm^{-1}$ and a saturation length of $15\ cm$ [74,85] is obtained.

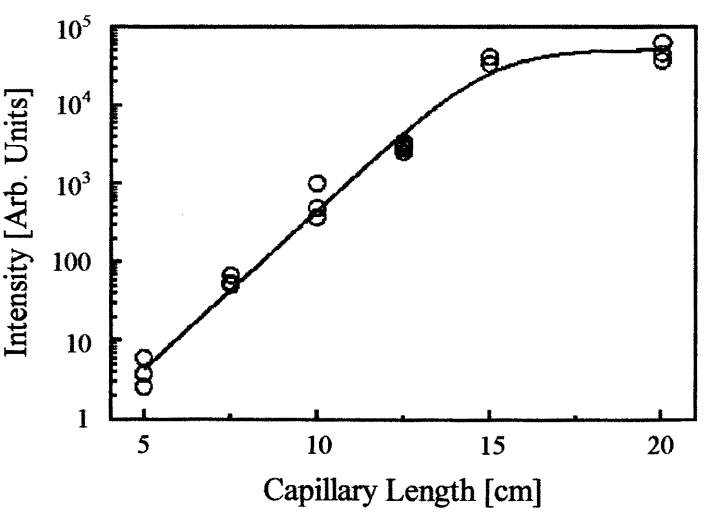

Figure1.4. Integrated intensity of the 46.9 nm line of Ne-like Ar as a function of plasma column length in a capillary discharge amplifier. The exponential increase of the intensity ceases at *l* ~15, where the saturation intensity is reached.

Direct excitation of plasma columns with an electrical discharge has the advantage of generating soft x-ray lasers that are very efficient and compact. Fast discharge excitation of capillary plasmas has produced the highest soft x-ray laser average power to date[8,86], 3.5 mW. In these lasers the electromagnetic forces of a fast current pulse flowing through a 3-4 mm diameter capillary channel rapidly compress the plasma to a column of about 300μm diameter. Figure 1.5 schematically illustrates the process that leads to the generation of laser radiation in the capillary channel. The fast current risetime minimizes the amount of material that is ablated from the capillary walls before the magnetic field detaches it from the walls[80-82,87,88].

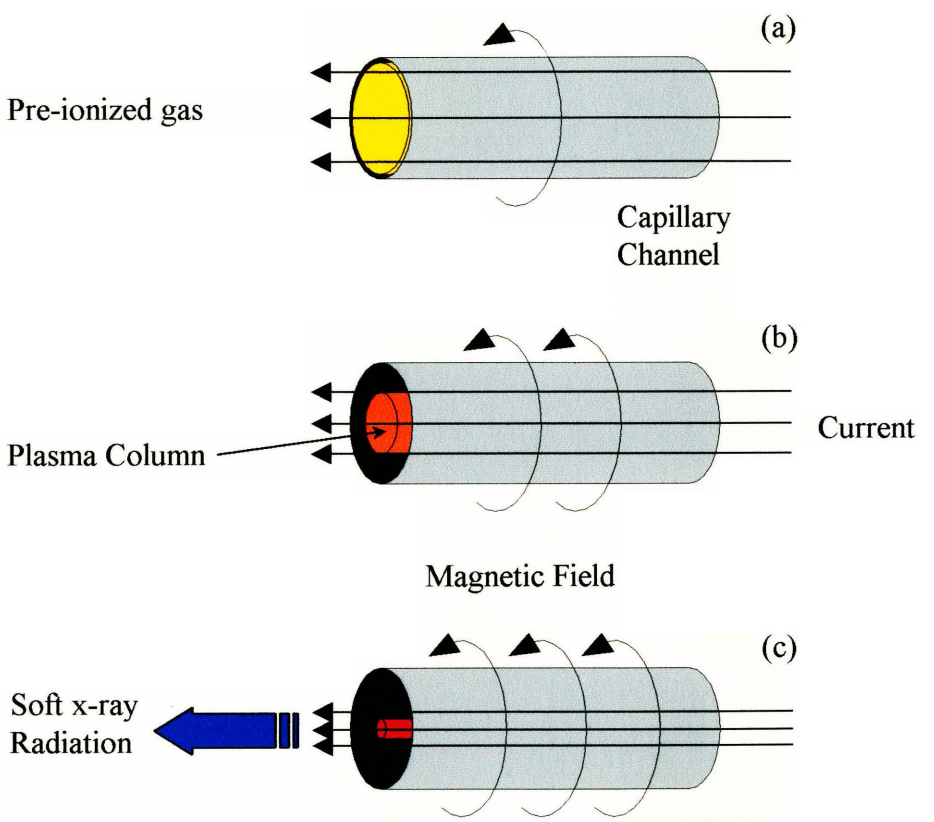

Figure 1..5. Scheme showing the steps in the generation of soft x-ray radiation from a discharge created plasma. (a) The gas is injected in the capillary channel and then pre-ionized. (b) The magnetic field produced by the current pulse compresses the plasma. (c) The soft x-ray radiation is obtained shortly before the time when the plasma column collapses (pinch), corresponding to a high density and high temperature plasma.

A very compact high repetition rate saturated 46.9 nm laser of size comparable to that of many widely utilized visible and ultraviolet gas lasers was developed utilizing the capillary discharge technology[8,83,86]. This laser was operated with capillaries 18.2 cm in length at a repetition rate of 7 Hz to produce an average output pulse energy of 135 μJ, corresponding to an average laser power of ~1 mW [86]. Increasing the plasma column length to 35.4 cm resulted in the generation of 0.88 mJ laser pulses at a repetition rate of 4 Hz, corresponding to an average power of 3.5 mW [8]. The spatially coherent average output power per unit bandwidth emitted by this compact laser at 26.5 eV is comparable to that one generated by a beam-line at a third generation synchrotron facility, while, its peak coherent power per unit bandwidth exceeds that of the synchrotron by several orders of magnitude[8,86].

These capillary discharge pumped table-top lasers were successfully used in several applications, including high resolution soft x-ray laser interferometry[89], shadowgraphy of plasmas[90], the measurements of XUV optical constants of materials[91], and the demonstration of laser ablation with a focused soft x-ray beam[92].

The Ne-like Ar results were extended to Ne-like S (60.8nm)[93]. To obtain amplification in Ne-like S, the discharge setup illustrated in Fig. 1.4 was modified to allow the sulfur vapor to be injected into the capillary channel through a hole in the ground electrode. The sulfur vapor was produced ablating the wall of an auxiliary capillary channel drilled in a sulfur rod by a slow current pulse. The generation of gain in Ne-like sulfur plasmas from a solid target using a table top capillary discharge proved the feasibility of producing amplification utilizing capillary discharge excitation schemes in

elements that are solid at room temperature. This is of vital importance in the attempt to extend this scheme to shorter wavelengths since scaling of collisionally excited capillary discharge lasers to wavelengths shorter than 46.9 nm, will require the use of elements heavier than Argon, leading into the metallic section of the periodic table.

The generation of coherent radiation at shorter wavelengths requires heavier elements to be ionized several times in order to observe transitions between high energy levels. As an illustrative example, while to obtain laser action in argon at 46.9 nm it is necessary to ionize the argon atoms eight times (Ar^{+8}), the generation of coherent radiation at 13.2 nm in cadmium requires the atoms to be ionized twenty times, and subsequently excited to the upper energy level, as shown in figure 1.1. The power density needed to accomplish such task is one to two orders of magnitude larger than the power density required to produce lasing in argon. Subsequently a new type of discharge configuration was designed to be able to deliver a very large amount of energy in very short period of time. This discharge scheme and the first results in capillary discharge-created metal vapor plasma are presented in chapter III of this thesis.

1.3. References

[1] D. T. Attwood, K. Halbach and N. J. Kim, Science, 228, 1264, (1985).

[2] D. T. Attwood, G. Sommargren, R. Beguiristain, K. Nguyen, J. Boker, N. Ceglio, K. Jackson, M. Koike, and J. Underwood, Appl. Opt. 32, 7022, (1993).

[3] R. Coisson, Appl. Optics, 34, 904, (1995).

[4] Free-Electron Laser Challenges, edited by P. G. O'Shea and H. E. Bennett, Proc. SPIE (Society of Photooptical Engineers, Bellingham, WA, 1997), Vol. 2988.

[5] Z. Chang, A. Rundquist, H. Wang, M. M. Murnane and H. C. Kapteyn, Phys. Rev. Lett. 79, 2967, (1997).

[6] A. Rundquist, C. G. Durfee III, Z. Chang, C. Herne, S. Backus, M. Murnane and H. C. Kapteyn, Science, 280, 1412, (1998).

[7] T. Ditmire, J. K. Crane, H. Nyugen, L. B. Da Silva and M. D. Perry, Phys. Rev. A, 51, R902, (1995).

[8] C. D. Macchietto, B. R. Benware and J. J. Rocca, Opt. Lett., 24, 1115, (1999).

[9] M. Frati, M. Seminario, and J. J. Rocca, Optics Letters, 25, 14, (2000).

[10] A. G. Molchanov, Sov. Phys. Usp, 15, 124, (1972).

[11] R. C. Elton, Appl. Optics, 14, 97, (1975).

[12] A. N. Zherikin, K. N. Koshelev and V. S. Letokhov, Sov. J. Quant. Electronics, 6, 82, (1976).

[13] A. V. Vinogradov, I. I. Sobel'man and E. A. Yukov, Sov. J. Quant. Electronics, 7, 32, (1977).

[14] L. A. Vainshtein, A. V. Vinogradov, V. I. Safranova and I. Vu. Skolev, Sov. J. Quant. Electronics, 8, 239, (1978).

[15] A. V. Vinogradov and V. N. Shlyaptsev, Sov. J. Quant. Electronics, 10, 753, 1980, and 13, 303, (1980).

[16] D. L. Matthews, et. al, Phys. Rev. Lett. 54, 110, (1985); M. D. Rosen, P. L. Hagelstein, D. L. Matthews, E. M. Campbell, A. U. Hazi, B. L. Whitten, B. MacGowan, R. E. Turner and R. W. Lee, Phys. Rev. Lett. 54, 106, (1985).

[17] R. C. Elton, "X-Ray Lasers," Academic Press, Boston, (1990).

[18] A. N. Zherikin, et al. Sov. J. Quant. Electron. 6, 82 (1976); A. V. Vinogradov and V. N. Shylyaptsev, Sov. J. Quant. Electron. 13, 303 and 1511 (1983).

[19] Y. Li, P. Lu, G. Pretzler, and E. E. Fill, Opt. Comm. 133, 196, (1997).

[20] D. J. Fields, et al., Phys. Rev. A 46, 1606, (1992).

[21] S. Maxon, P. Hagelstein, B. MacGowan, R. London, M. Rosen, J. Scofield, S. Halhed

and M. Chen, Phys. Rev. A 37, 2227 (1988); also, W. H. Goldstein, J. Oreg, A. Zigler, A. Barshalom, and M. Klapisch, Phys. Rev. A 38, 1797 (1988).

[22] B. J. MacGowan, S. Maxon, L. B. DaSilva, D. J. Fields, C. J. Keane, D. L. Matthews, A. L. Osterheld, J. H. Scofield, G. Shimkaveg, and G. F. Stone, Phys. Rev. Lett. 65, 420 (1990).

[23] B. J. MacGowan et al., Phys. Rev. Lett. 65, 2374, (1990).

[24] R. Smith, G. J. Tallents, J. Zhang, S. McCabe, C. J. Pert, and E. Wolfrum, Phys. Rev. A, 59, R47, (1999).

[25] P. L. Hagelstein, Proc. OSA Meeting on Short Wavelength Coherent Radiation: Generation and Applications, edited by R. W. Falcone and J. Korz, 1988 p.28; Proc. SPIE 1551, 254 (1991)

[26] B. J. MacGowan et al., J. Appl. Phys. 61, 5245, 1987.

[27] B. J. MacGowan, S. Maxon, P. L. Hagelstein, C. J. Keane, R. A. London, D. L. Matthews, M. D. Rosen, J. H. Scofield and D. A. Whelan, Phys. Rev. Lett. 59, 2157, 1987.

[28] T. N Lee, E. A. McLean and R. C. Elton, Phys. Rev. Lett. 59, 1185, 1987.

[29] B. J. MacGowan, S. Maxon, C. J. Keane, R. A. London, D. L. Matthews and D. A. Whelan, J. Opt. Soc. Am. B5, 1858, (1988).

[30] A. Carillon et al., Phys. Rev. Lett., 68, 2917, (1992).

[31] D. M. O'Neill, C.L.S. Lewis, D. Neely, J. Uhomopbhi, M. H. Key, A. MacPhee, G. J. Tallents, S. A. Ramsden, A. Rogovski and E. A. McLean, Opt. Comm. 75, 406 (1990).

[32] B. J. MacGowan et al., Phys. Fluids B 4, 2326, (1992).

[33] C.J. Keane et al. Phys. Rev. A 42, 2327, (1990).

[34] P. L. Hagelstein, Plasma Physics, 25, 1345, (1983), and "Atomic Physics 9", P. 382, Ed. R. S. Van Dyck Jr. and E. N Fortson, World Sci. Publ., Singapore, (1984).

[35] J. G. Lunney, Appl. Phys. Lett. 46 891 (1986).

[36] C. L. S. Lewis, et al., Opt. Comm. 91, 71 (1992).

[37] R. Kodama, D. Neely, Y. Kato, H. Daido, K. Murai, G. Yuan, A. MacPhee, and C.L.S. Lewis, Phys. Rev. Lett. 73, 3215 (1994).

[38] Wanshiji, et al., J. Opt. Soc. Am. B 9, 360, (1992).

[39] I. T. Boehly et al., Phys. Rev. A 42, 6962, (1990).

[40] J. Nilsen, B. J. MacGowan, L. B. Da Silva, and J. C. Moreno, Phys. Rev. A 48, 4682,

(1993).

[41] S. Basu, P. L. Hagelstein, J. G. Gooberlet, M. H. Muendel and S. Kaushik, Appl. Phys. B. 57, 203, (1993).

[42] J. Nilsen, J. C. Moreno, L. B. DaSilva and T. W. Barbee Jr., Phys. Rev. A 55, 827, (1997).

[43] J. C. Moreno, J. Nilsen, Y. L. Li and E. E. Fill, Opt. Lett. 21, 866, (1996).

[44] J. Nilsen and J. C. Moreno, Phys. Rev. Lett. 74, 3376, (1995).

[45] A. R. Prag, A. Glinz, J.A. Balmer, Y. Li, and E.R. Fill. Appl. Phys. B 63, 113, (1996).

[46] G. F. Cairns, et al., Opt. Commun. 124, 777-789, (1996).

[47] Y. Li, G. Pretzler and E. E. Fill, Phys. Rev. A 52, R3433, (1995), and E. F. Fill, Y. Li, D. Schlögl, J. Steingruber and J. Nilsen, P. 134 in Ref. 71.

[48] H. Daido, R. Kodama, K. Murai, G. Yuan, M. Takagi, Y. Kato, I. W. Choi, and C. H. Nam, Opt. Lett. 20, 61, (1995).

[49] B. Rus, A. Carillon, P. Dhez, P. Jaeglé, G. Jamelot, A. Klisnick, M. Nantel, and P. Zeitoun, Phys. Rev. A 55, 3858, (1997).

[50] J. Nilsen, J.C. Moreno, B.J. Moreno, B.J. MacGowan, and J.A. Koch. Appl. Phys. B 57, 309, (1993).

[51] E. E. Fill, Y. Li, D. Schlögl, J. Steingruber and J. Nilsen, Opt. Lett. 20, 374, (1995).

[52] G. J. Tallents, P. 30 in Ref. 69.

[53] J. C. Moreno, J. Nilsen and L. B. DaSilva, Opt. Comm., 110, 585, (1994).

[54] J. Nilsen, Y. Li, P. Lu, J. C. Moreno, and E. E. Fill, Opt. Comm. 124, 287, (1996).

[55] Y. L. Li, G. Pretzler, P. X. Lu, E. E. Fill, and J. Nilsen, Phys. Plasmas, 4, 479, (1997).

[56] G. Yuang, K. Murai, H. Daido, R. Kodama and Y. Kato, Phys. Rev. A52, 4861, (1995).

[57] J. Zhang, et al., Phys. Rev. A 53, 3640, (1996).

[58] J. Zhang et al. Phys. Lett. A 234, 410, (1997).

[59] A. R. Prag, F. Loewenthal, and J. E. Balmer, Phys. Rev. A 54, 4585, (1996).

[60] R. Tomassini, F. Lowenthal and J. E. Balmer, Phys. Rev. A 59, 1577 (1999).

[61] F. Lowenthal, R. Tommasini and J. E. Balmer, Opt. Comm. 154, 325, (1998).

[62] H. Daido et. al., Phys. Rev. Lett. 75, 1074 (1995).

[63] H. Daido et. al., Opt. Lett. 21, 958 (1996).

[64] J. Zhang, et al., Phys. Rev. Lett. 78, 3856, (1997).

[65] J. Zhang, et al., Science, 276, 1097, (1997).

[66] J. Zhang, et al., P. 53 in Ref. 69.

[67] J. Zhang, et al., Phys. Rev. A, 54, R4653, (1996).

[68] R. Smith, G. J. Tallents, J. Zhang, G. Eker, S. McCabe, G. J. Pert, and E. Wolfrum, Phys. Rev. A 59, R47, (1999).

[69] Yu. A. Afanasiev and V. N. Shlyaptsev, Sov. J. Quantum Electron, 19, 1606, (1989).

[70] V. N. Shlyaptsev, P. V. Nickles, T. Schlegel, M. R. Kalashnikov and A. L. Osterheld, P. 111 in Ref. 61; V. N. Shlyaptsev, J. J. Rocca, M. P. Kalashnikov, P. V. Nickles, W. Sandner, A. L. Osterheld, J. Dunn and D. C. Eder, P. 93 in Ref. 69; C. D. Decker and R. A. London, P. 94 ibid,; J. Nilsen, P. 86 ibid.

[71] P. V. Nickles, V. N. Shlyaptsev, M. Kalashnikov, M. Schnurer, I. Will and W. Sandner, Phys. Rev. Lett., 78, 2748, (1997).

[72] J. Dunn, A. L. Osterheld, R. Shepherd, W. E. White, V. N. Shlyaptsev and R. E. Stewards, Phys. Rev. Lett. 80, 2825, (1998).

[73] J. Dunn, A. L. Osterheld, R. Shepherd, W. E. White, V. N. Shlyaptsev, A. Bullock, and R. E. Stewart, P. 114 in Ref. 69.

[74] M. P. Kalachnikov et al., Phys. Rev. A 57, 4778 (1998).

[75] J. Dunn, Y. Li, A. L. Osterheld, J. Nilsen, J. R. Hunter, and V. N. Shlyaptsev, Phys. Rev. Lett. 84, 4834, (2000); and J. Dunn, Y. Li, A. L. Osterheld, J. Nilsen, S. J. Moon, K. B. Fournier, J. R. Hunter, A. Ya. Faenov, T. A. Pikuz and V. N. Shlyaptsev. P. 2 in Ref. 67; J.Dunn, J. Nilsen, A.L. Osterheld, Y. Li, and V.N. Shlyaptsev . Opt. Lett. 24, 101, (1999).

[76] C.L.S. Lewis, et al., P. 292, Ref. 67.

[77] J. L. Miquel, N. Blanchot, L. Bonnet, S. Jacquemot, A. Klisnick, J. Kuba, D. Ros, P. Fourcade, G. Jamelot, F. Dorchies, J. C. Chanteloup, P. 24, ibid.

[78] B. E. Lemoff, G. Y. Yin, C. L. Gordon III, C.P.J. Barty and S. E. Harris, Phys. Rev. Lett., 74, 1576, (1995) and S.M. Hooker, P.T. Epp and G. Y. Yin , J. Opt. Soc. Am. B. 14, 2735, (1997).

[79] J. J. Rocca, D. C. Beethe and M. C. Marconi, Opt. Lett., 13, 565, (1988).

[80] J. J. Rocca, V. Shlyaptsev, F. G. Tomasel, O. D. Cortázar, D. Hartshorn, and J.L.A.

Chilla, Phys. Rev. Lett. 73, 2192-2195, (1994).

[81] J. J. Rocca, F. G. Tomasel, M. C. Marconi, V. N. Shlyaptsev, J. L. A. Chilla, B. T. Szapiro and G. Guidice, Phys. of Plasmas 2, 2547, (1995).

[82] J. J. Rocca, D. P. Clark, J.L.A. Chilla, and V. N. Shlyaptsev, Phys. Rev. Lett. 77, 1476-1479, (1996).

[83] B. R. Benware, C. H. Moreno, D. J. Burd and J. J. Rocca, Opt. Lett. 22, 796, (1997).

[84] G. J. Linford, E. R. Peresini, W. R. Soor and M. L. Spaeth, Appl. Optics, 13, 379, (1974).

[85] "X-Ray Lasers 1996," Eds. S. Svanberg and C. G. Wahlstrom, (Institute of Physics, Bristol, (1996).

[86] B. R. Benware, C. D. Macchietto, C. H. Moreno, and J. J. Rocca, Phys. Rev. Lett. 81, 5804, 1998.

[87] J. J. Rocca, O. D. Cortázar, B. Szapiro, K. Floyd and F. G. Tomasel, Phys. Rev. E, 47, 1299, (1993).

[88] J. J. Rocca. M. C. Marconi, J.L.A. Chilla, D. P. Clark, F. G. Tomasel and V. N. Shlyaptsev, IEEE J. of Sel. Topics in Quant. Elect. 1, 945, (1995).

[89] J. J. Rocca, C. H. Moreno, M. C. Marconi, and K. Kanizay, Opt. Lett. 24, 240, (1999); C. H. Moreno, M. C. Marconi, K. Kanizay, J. J. Rocca, Yu. A. Unspenskii, A. V. Vinogradov and Yu A. Pershin, Phys. Rev. E, 60, 911, (1999); J. Filevich, M. Marconi, K. Kanizay, J.L.A. Chilla and J.J. Rocca. Opt. Lett. 25, 5, 356, (2000).

[90] C. H. Moreno, M. C. Marconi, V. N. Shlyaptsev, and J. J. Rocca, IEEE Trans. Plasma Sci. 27, 6, (1999).

[91] I. A. Artioukov, B. R. Benware, J. J. Rocca, M. Forsythe, Yu. A. Uspenskii and A. V. Vinogradov, IEEE. J. Sel. Topics in Quant. Elect. 5, 1495, (1999).

[92] B. R. Benware, A. Ozols, J. J. Rocca, I. A. Artioukov, V. V. Kondratenko, and A. V. Vinogradov, Opt. Lett. 24, 1714, (1999).

[93] F. G. Tomasel, J. J. Rocca, V. N. Shlyaptsev, and C. D. Macchietto, Phys. Rev. A 55, 437, (1997).

[94] N. Yamaguchi, T. Hara, C. Fujikawa, and Y. Hisada, Jpn. J. Appl. Phys., part 2 36, L 1297 (1997).

[95] S. M. Hooker, P. T. Epp, and G. Y. Yin, J.Opt. Soc. Am. B 14, 2735 (1997).

CHAPTER II

DEVELOPMENT OF 10 MICRO-JOULE TABLETOP LASER AT 52.9 NM IN NE-LIKE CHLORINE.

2.1. Introduction

There is much interest in the demonstration of practical XUV and soft x-ray lasers that would offer a variety of wavelengths for applications. As discussed in the previous chapter, several laser excitation schemes for the development of tabletop short wavelength lasers, based on the excitation by optical lasers or fast capillary discharges, are currently under investigation[1-12]. While gain has been demonstrated in a large number of transitions, to date, only a few compact short wavelength lasers have been reported to produce laser pulse energies greater than $1\,\mu J$. These include a capillary discharge pumped 46.9 nm Ne-like Ar laser that has produced average output pulse energies of $0.88\,mJ$ at 4 Hz repetition rate[11], and laser-pumped transient inversion lasers in Ni-like Pd at 14.7 nm and Ni-like Mo at 18.9 nm, that have produced output pulse energies of about $10\,\mu J$ and $2-5\,\mu J$ respectively, at repetition rates of one shot every 4 minutes[8]. There is significant interest in extending the availability of practical tabletop short

wavelength lasers to other wavelengths. In particular, applications in photochemistry and photophysics can significantly benefit from laser sources of high energy photons that are capable of single-photon ionization of any neutral specie, yet fall short of the 24.6 eV corresponding to the He photoionization threshold. These applications include the study of nanoclusters created by optical laser ablation, a technique that uses He as a carrier gas[13].

In this chapter, the generation of laser pulses at 52.9 nm (23.4 eV) in the $3p\,^1S_0$ - $3s\,^1P_1$ transition of Ne-like Cl utilizing a very compact tabletop capillary discharge is discussed. Figure 2.1. is an energy level diagram of Ne-like Cl showing the laser transition. Laser amplification of this line was previously observed by Y. Li et al. in a plasma generated by exciting a solid KCl target with $450 \pm 20\ J$ laser pulses of 0.45 ns duration produced by the powerful Asterix iodine laser facility at a rate of several shots per hour[14]. In that experiment the amplification obtained in a 3 cm long plasma (gl ~ 7.5) was far below that required to reach gain saturation, limiting the laser pulse output energy to relatively low values. In the 18.2 cm long discharge-pumped plasma column used in the experiments reported in this thesis the amplified spontaneous emission intensity reached values of the order of the saturation intensity, allowing for the generation of a significantly greater laser output pulse energy. Laser pulses with energy up to $10\ \mu J$ were measured operating the discharge at rates between 0.5 and 1 Hz. Moreover, the results were obtained with a very compact tabletop device of size comparable to some of the most widely used visible and ultraviolet gas lasers.

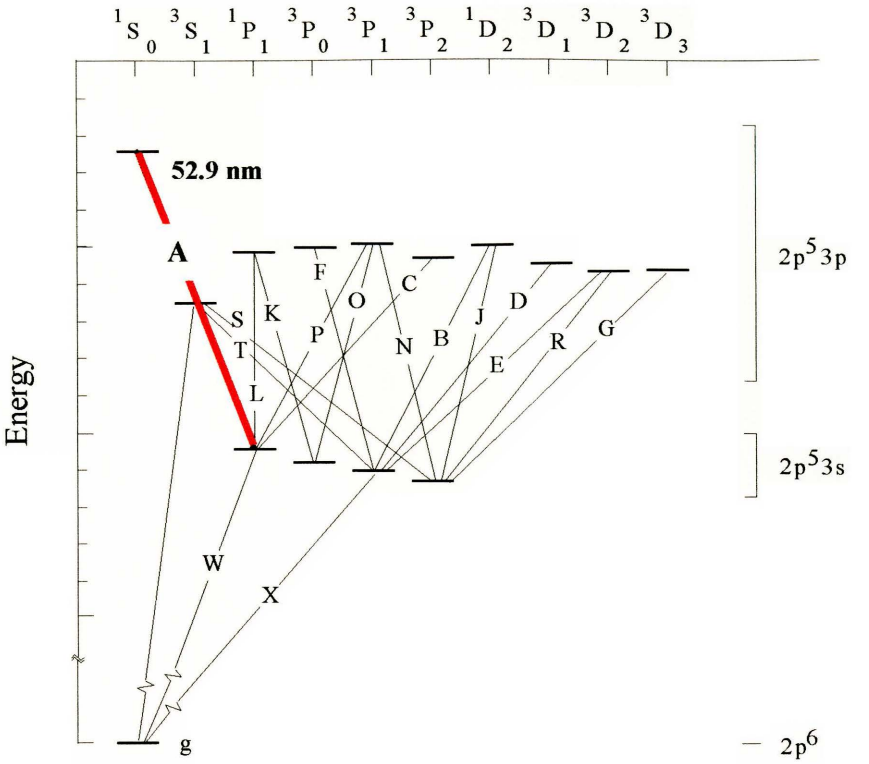

Figure 2.1. Energy level diagram for Ne-like Cl. The red line shows the laser transition between the energy levels $3p\,^1S_0$-$3s\,^1P_1$.

2.2. Experimental setup

Although the capillary discharge set up utilized in the experiment is similar to that previously used to obtain lasing in Ne-like Ar at high repetition rates[10], special care had to be taken to protect the detection and diagnostics equipment from the corrosive effect of Cl_2. The chlorine gas was continuously admitted into the capillary channel using

chemically compatible Teflon tubing and stainless steel fittings. The gas was pumped using a rotary vane pump containing perfluoropolyether oil and turbomolecular pumps purged with N_2. An aluminum filter 1400 Å thick was placed between two turbomolecular pumps to isolate the laser from the detection system. Figure 2.2. shows a scheme of the setup utilized in the experiment.

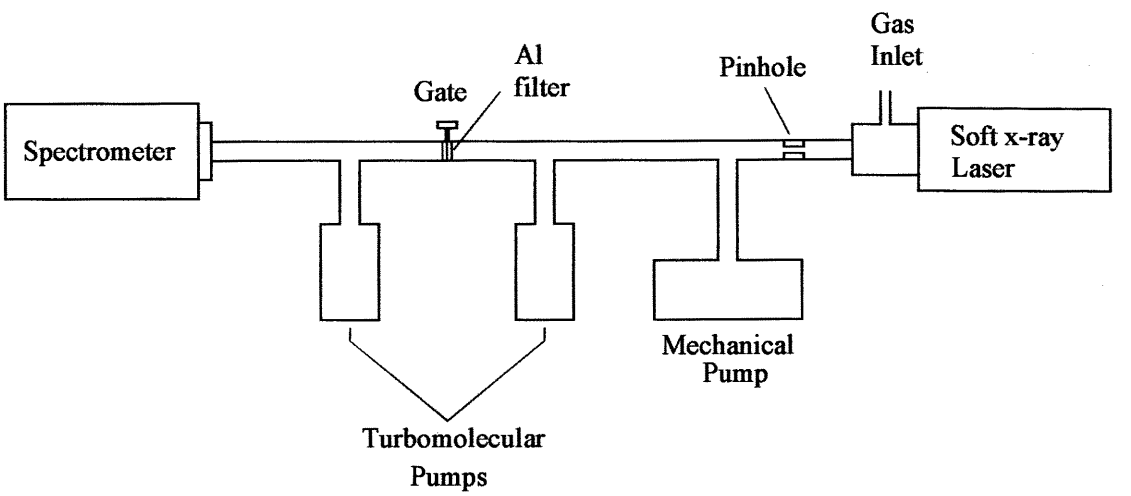

Figure 2.2. Scheme of the experimental setup utilized for the demonstration of the chlorine laser. The figure shows the differential pumping stage used to isolate the detection system from the corrosive effects of the chlorine gas.

The gain media, consisting of a plasma column of the above mentioned length, was generated by rapidly exciting a 3.2 mm inside diameter aluminum oxide capillary channel filled with pre-ionized chlorine gas with a fast current pulse. Amplification was observed at Cl_2 pressures ranging from 120 to 300 mTorr. The plasma columns were excited by current pulses of approximately 23 kA peak amplitude, 10-90 % rise-time of

approximately 25 ns, and first half cycle duration of 110 ns. In this discharge, the fast current pulse rapidly compresses the plasma creating a small diameter column[1,5] in which monopole collisional electron excitation of Ne-like Cl ions creates a large population inversion between the $3p\,^1S_0$ and $3s\,^1P_1$ levels, resulting in strong amplification at 52.9 nm.

Spectral diagnostic was implemented utilizing a 1m focal length normal incidence spectrograph containing a 600 l/mm diffraction grating. The detector consisted of two microchannel-plates (MCP) in a chevron configuration, a phosphorus screen and a charged-coupled device (CCD) detector array. The front MCP, coated with magnesium oxide to enhance the photoelectron response, was voltage pulsed in order to perform time resolved measurements.

2.3. Experiment and results

In order to detect and demonstrate laser action, time resolved spectra were obtained covering the vicinity of the laser transition. Figure 2.3. shows spectra of the axial emission of the discharge, covering a 40 nm region in the vicinity of the $J = 0 - 1$ laser line of Ne-like Cl. The spectrum obtained at a pressure of 120 mTorr (Fig. 2.3.a), shows line emission at the 52.9 nm wavelength of the laser transition. However, at this pressure, the intensity of this line is weak, smaller than that of several neighboring transitions of ClVI and ClVII, which cannot be inverted. A dramatic change in the spectrum was observed when the pressure was adjusted to 224 mTorr, the optimum pressure for lasing (Fig. 2.3.b). At this pressure, the laser line is over two orders of magnitude more

intense and completely dominates the entire 40 nm wide spectrum. This is clear evidence of large amplification in the 52.9 nm line.

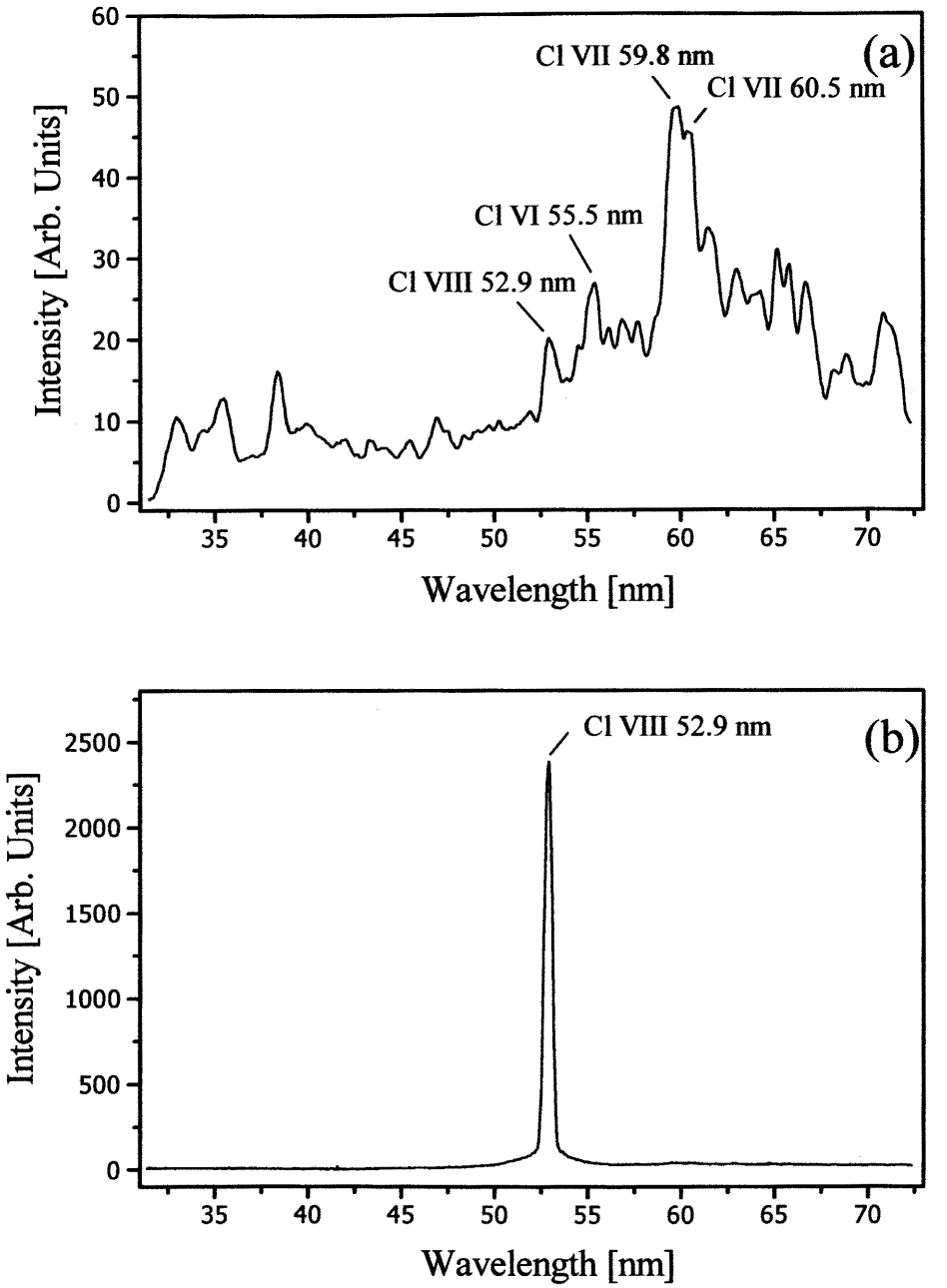

Figure 2.3. On-axis emission spectra of the Cl capillary discharge plasma in the region between 30 and 70 nm. (a) spectrum corresponding to a 120 mTorr discharge. (b) spectrum corresponding to a 224 mTorr discharge. In the latter, the dominance of the 52.9 nm Ne-like Cl transition is a clear indication of strong amplification.

The most common way to characterize the performance of XUV and soft x-ray lasers is the measurement of the gain of the integrated laser line intensity as a function of plasma column length. However, since in our case the laser output intensity was observed to be high, we could afford to directly measure the laser output energy which is of higher practical interest for applications. The energy and temporal evolution of the laser output pulse were monitored with a vacuum photodiode placed at a distance of 90 cm from the exit of the laser. The data was recorded and stored by a 2 Gs/s digitizing oscilloscope with 500 MHz analog bandwidth. The efficiency of the aluminum photocathode was previously calibrated with respect to a silicon photodiode of known quantum efficiency[5]. To avoid saturation of the photodiode, the laser output was attenuated with a stainless steel mesh of measured transmissivity. Figure 2.4. shows a laser pulse with energy of $10\ \mu J$ measured operating the system at a repetition frequency of 0.5 Hz. For an accurate measurement of the laser pulsewidth we utilized a fast vacuum photodiode and a 1Ghz bandwidth analog oscilloscope. The laser pulsewidth was obtained by correcting the measured signal for the response of the detection system. The measurement of multiple shots yielded an averaged laser full width half maximum (FWHM) pulse of 1.56 ± 0.25 ns. The corresponding peak power is approximately 7 kW. However, the shot to shot variation in the laser pulse energy was significantly larger than those measured operating the laser at 46.9 nm using Ar[10,11]. The laser output pulse energy was also observed to be significantly deteriorated at repetition rates greater than 1 Hz. This is probably due to insufficient gas renewal in the capillary channel, in which the reactive nature of excited Cl_2 gas leads to the buildup of contaminants.

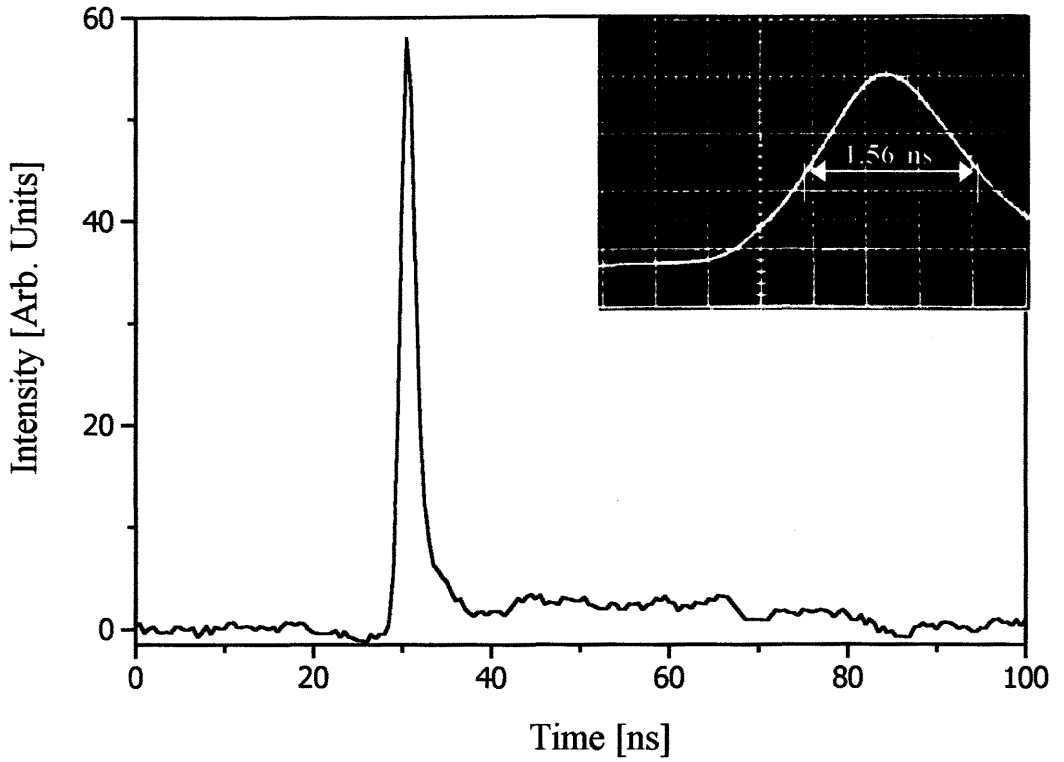

Figure 2.4. Temporal evolution of the laser output pulse. The insert in the top right corner corresponds to the signal recorded with a fast vacuum photodiode and a 1-GHz bandwidth analog oscilloscope. The signal corrected for the limited bandwidth of the detection system yields a laser FWHM pulsewidth of 1.56 ns.

A direct measurement of the beam divergence was also obtained by recording the far-field pattern of the laser beam. The laser beam profiles were recorded using a detector composed of a MCP, a phosphorus screen and a CCD, placed at 97 cm from the end of the capillary. The MCP was gated for about 5 ns to minimize the background signal resulting from the long lasting spontaneous emission radiated by hundreds of spectral lines excited by the discharge. The laser beam was attenuated by the Al-Si filter that was

again used to protect the MCP from Cl_2 gas. Figure 2.5. illustrates the far field beam profile measured at optimum discharge conditions. The beam was observed to present maximum intensity on axis, and a FWHM divergence of approximately 4 mrad.

The next chapter discusses the results of the work conducted utilizing a high power capillary discharge developed with the purpose of extending capillary discharge pumped soft x-ray lasers to shorter wavelengths.

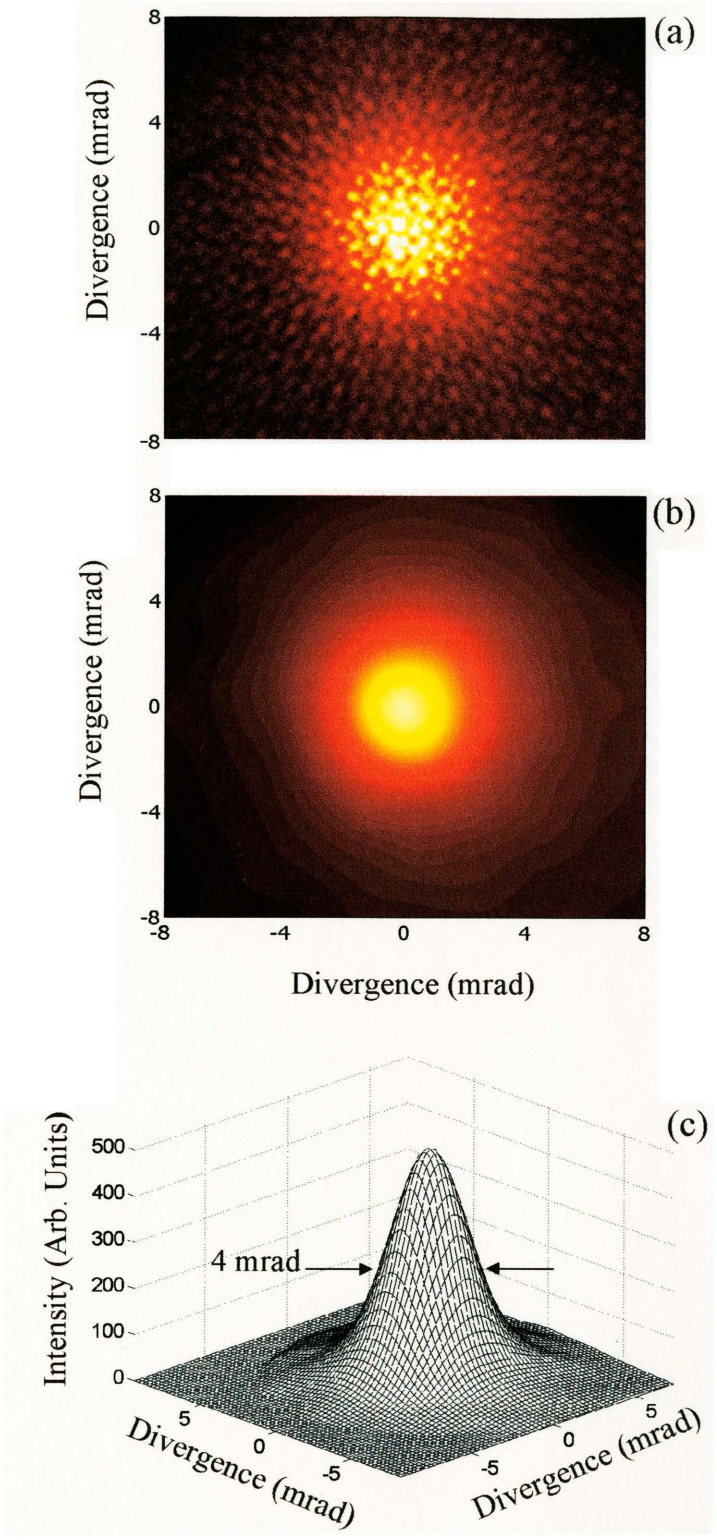

Figure 2.5. Far field profile of the chlorine laser pulse corresponding to a Cl pressure of 224 mT and a current peak of 23 kA. (a) Picture of the beam at 94 cm from the output. The pattern observed is due to the mesh used to sustain the 1400 Å filter. (b) Same image after filtering. (c) 3-D plot of the beam profile.

2.4. References

[1] J.J. Rocca, V.N. Shlyaptsev, F.G. Tomasel, O.D. Cortazar, D. Hartshorn, and J.L.A. Chilla. Phys. Rev. Lett., **73**, 2192 (1994).

[2] B.E. Lemoff, G.Y. Yin, C.L. Gordon III, C.P.J. Barty, and S.E. Harris, Phys. Rev. Lett., **74**, 1576 (1995).

[3] D. Korobkin, C.H. Nam, S. Suckewer and A. Golstov, Phys. Rev. Lett, **77**, 5206 (1996).

[4] F.G. Tomasel, J.J. Rocca, V.N. Shlyaptsev, and C.D. Macchietto. Phys. Rev E. 55, 1437, (1996)

[5] J.J. Rocca, D.P. Clark, J.L.A. Chilla and V.N. Shlyaptsev, Phys. Rev. Lett., **77**, 1476 (1996).

[6] P.V. Nickles, V.N. Shlyaptsev, M. Kalashnikov, M. Schnurer, I. Will, and W. Sandner, Phys. Rev. Lett., **78**, 2748 (1997).

[7] J. Dunn, A.L. Osterheld, S. Sheperd, W.E. White, V.N. Shlyaptsev, and R.E. Stewards, Phys. Rev. Lett., **80,** 2825 (1998).

[8] J. Dunn, Y. Li, A.L. Osterheld, J. Nilsen, S.J. Moon, K.B. Fournier, J.R. Hunter, A.Ya. Faenov, T.A Pikuz and V. N. Shlyaptsev. Proc. SPIE 3776, 2 (1999)

[9] D. Korobkin, A. Goltsov, A. Morozov, and S. Suckewer, Phys. Rev. Lett. **77**, 1476 (1998).

[10] B. R. Benware, C.D. Macchietto, C.H. Moreno and J.J. Rocca, Phys. Rev. Lett., **81**, 5804 (1998).

[11] C. D. Macchietto, B. R. Benware and J. J. Rocca, Opt. Lett., **24**, 1115 (1999)

[12] R. Tommasini, F. Lowenthal and J.E. Balmer, Phys. Rev. A, **59,** 1577 (1999).

[13] M. Foltin, J. G. Stuber and E. R. Bernstein, J. Chem. Phys. **III**, 9577 (1999); and results on ZrO_2 clusters (unpublished).

[14] Y. Li, G. Pretzler and E. E. Fill, Phys. Rev. A, **52**, R3433 (1995).

CHAPTER III

STEPS TOWARDS THE DEVELOPMENT OF CAPILLARY DISCHARGE LASERS AT SHORTER WAVELENGTHS

3.1. Introduction

In the previous chapter the demonstration of a 52.9 nm laser in Ne-like Cl (seven times ionized Cl) was discussed. The generation of lasers at shorter wavelengths requires heavier elements to be ionized several times in order to obtain higher energy level transitions.

Although the Ne-like isoelectronic sequence $\left(1s^2\ 2s^2\ 2p^6\right)$ has proven to be successful in the creation of laser transitions[1], a faster scaling to shorter wavelengths is obtained using higher Z atoms in the Ni-like configuration as it can be seen in figure 3.1. Lasing in Ni-like ions takes place in $\Delta n = 0$ transitions between $n = 4$ levels[2].

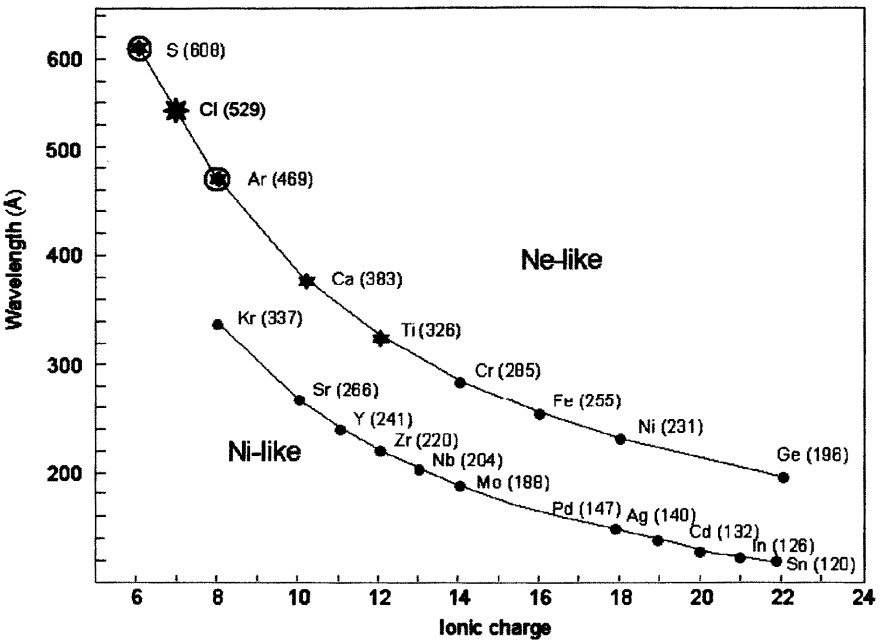

Figure 3.1. Plot showing the scaling of the wavelength with the ionic charge (Z) for Ne-like and Ni-like ions.

As discussed in the next section we selected cadmium vapor plasma as possible gain medium of Ni-like ions. This chapter discusses preliminary studies related to the possibility of observing gain at 13.2 nm in a capillary discharge created plasma using these ions.

3.2. Motivation and approach

There is a particular interest in the election of cadmium as the amplification medium for soft x-ray lasers and it resides on the facts that cadmium can be easily vaporized, and it has the right energy level configuration to obtain laser radiation in the transition $4d\ ^1S_0$ - $4p\ ^1P_1$ in Ni-like Cd at 13.2 nm. This wavelength, considerably

shorter than 46.9 nm obtained in Ne-like Ar[3], has a significant importance for EUV lithography.

In order to obtain gain in a Cd vapor medium at 13.2 nm, plasmas with electron temperature greater than 300 eV and density around $10^{20}\ cm^{-3}$ need to be generated. This plasma conditions require a much larger power density deposition than that produce in the Ne-like Cl experiment, which can in principle be obtained increasing the discharge current. However, in capillary discharge-created plasmas, an increment in the excitation current does not necessarily result in a significantly higher plasma temperature, as more material is ablated from the walls. For example, high current pulses of 500 kA and 300 ns rise time injected through narrow capillary channels have created high density but very cold plasmas (Te = 10 eV), which have been used for the study of transport coefficients in partially degenerated, strongly coupled plasmas[4]. Under this conditions, the material injected into the plasma by wall ablation limits the temperature to relatively low values. The key to generate a hot plasma in a capillary discharge consists in depositing a very large energy density during a very short period of time. A fast rise of the current allows to rapidly decouple the plasma from the capillary walls. For this purpose, a new high power fast capillary discharge set up was designed and implemented[5].

3.3. Development of high power pulse generator and capillary discharge

As mentioned in the previous section, in order to create the conditions for a short wavelength laser emission to occur in a capillary discharge created plasma, a large and

very fast current pulse must be generated. In order to supply a high power density, the three-stage pulse compression scheme, shown in figure 3.2., was developed[5]. The three segments of the setup, in the direction of the traveling current pulse, are a Marx generator, a water capacitor and a Blumlein transmission line.

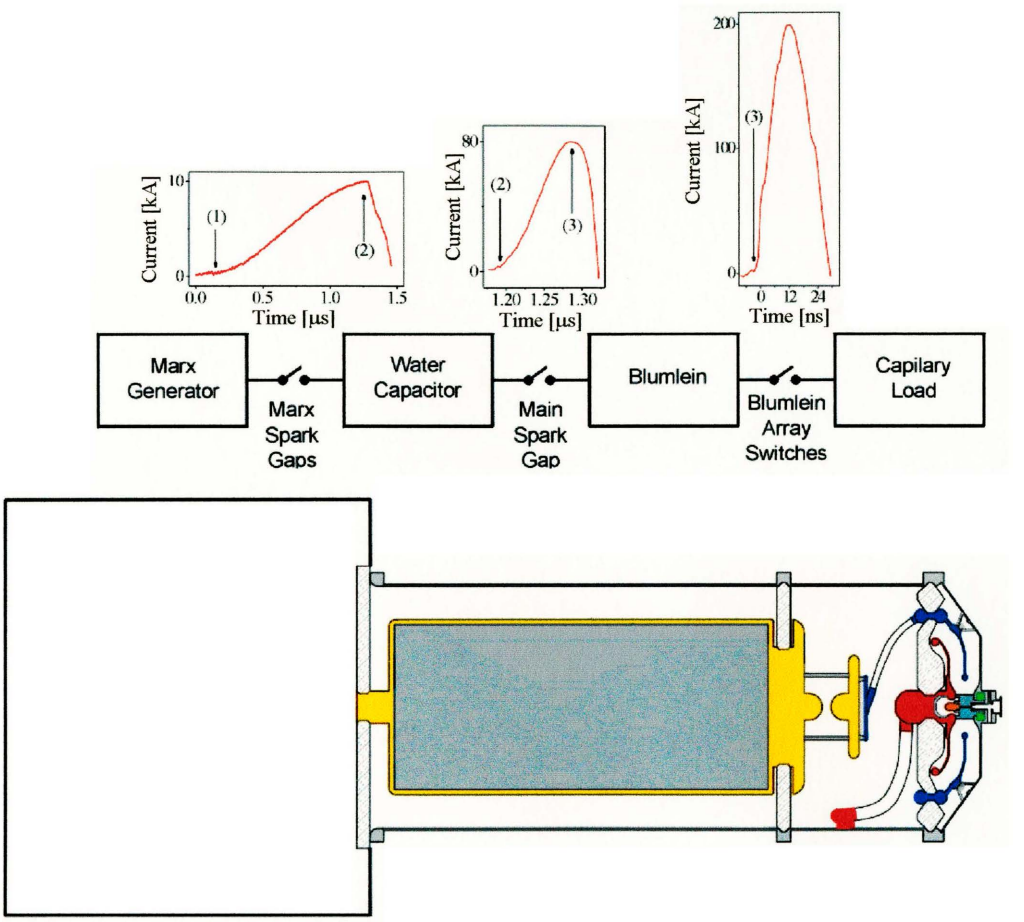

Figure 3.2. Schematic illustration of the pulse compression scheme to produce high power electrical pulses by successive transfer of energy, operating principle and the observed outputs of the current generator. The arrows indicate the relative time at which the different switches are closed.

Each of the three pulse compression stages are separately discussed below.

3.3.1 Marx generator

The first block from the left in figure 3.2 represents a Marx generator. In this case consists of eight capacitors separated by eight spark-gap switches. In normal operation, these capacitors are charged in parallel and discharged in series generating at the output eight times the charging voltage.

The Marx generator is the initial energy storage medium, converting the DC current from the charging power supply, in the milliampere range, into a $10\ kA, 1.3\ \mu s$ rise time current pulse. When operated fully charged, it delivers peak voltage pulses of 800 kV. In the experiments reported herein, each of the eight stages of the Marx was charged to 70 kV, giving an output voltage of 560 kV. The current pulse created by the Marx generator is used to charge the water capacitor that constitutes the second stage of pulse compression.

3.3.2. Water capacitor

The second compression process makes use of a water capacitor (shown in the central part of fig. 3.2). This part of the setup consists in a coaxial capacitor 1 m in diameter that uses water as a dielectric, and which has a total capacitance of $26\ nF$. The purpose of this stage is to significantly shorten the duration of the pulse generated by the Marx to create a narrower current pulse that can rapidly charge the third and last stage. This compression is achieved by drastically reducing the inductance between one stage

and the next. The water capacitor is connected to a self-triggered spark-gap switch that once closed produces a ~80 *kA*, 100 *ns* rise time current pulse.

3.3. 3. Blumlein transmission line

The final compression stage is a Blumlein transmission line consisting of three circular parallel plates and seven radially arranged spark gap switches.

The basic structure of a Blumlein transmission line may be viewed as two simple transmission lines connected in a way such that they are charged in parallel and discharged in series. This configuration can produce an output voltage twice as high as that of a simple transmission line on an open load. An equivalent circuit is shown in figure 3.3.

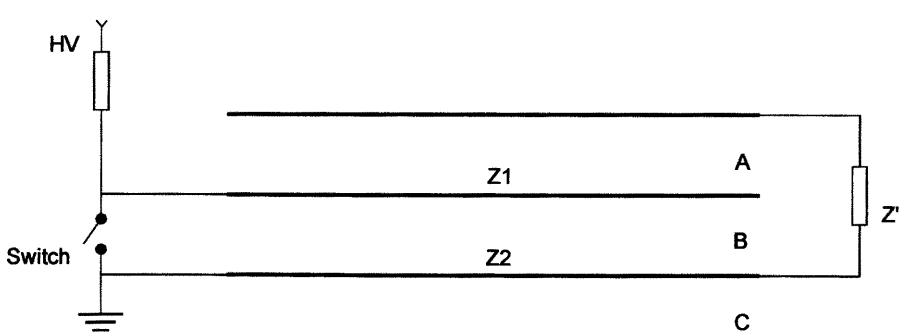

Figure 3.3. Equivalent circuit for a Blumlein transmission line in parallel-plates configuration, A= upper plate, B = middle plate, C = lower plate; Z1, Z2 = characteristic impedance of upper and lower lines; Z' = load impedance.

A Blumlein transmission line can be constructed either in cylindrical form or in a parallel plate configuration. In parallel plate form, its basic structure mainly consists of three parallel plates arranged in the configuration shown in figure 3.4. For operation at very high voltages the space between the plates is filled with a liquid dielectric medium, such as oil or de-ionized water. Between the middle (B) and lower plate (C) there is a switch to control the discharge of the line. The distance between the plates and the width of the plates is chosen to obtain the desired characteristic impedance while maintaining the electric field below the value of dielectric breakdown. The load (Z') is commonly connected between the lower (C) and the top (A) plate. The high voltage input (HV) that charges the line is fed in via the middle plate. In our implementation, however, the plates are circular, the capillary load is placed at the axis, and several spark gaps are distributed along the periphery as shown in figure 3.4.

The motivation for using a circular array of seven spark-gaps is to obtain a very low switching inductance resulting in a very fast output current pulse rise time. Moreover it is necessary to provide a symmetric and synchronized switching of the transmission line. This produces a radially symmetric electromagnetic wave that rapidly advances towards the center of the circular parallel plates, generating a fast current pulse on the load located at the axis of the discharge. It should be noticed that an asynchronous firing of the switches would result in a broadening of the current pulse. Once the current pulse leaves the last compression stage its rise time is reduced a hundred times respect to the original pulse generated by the Marx generator (from $\approx 1\,\mu s$ to $\approx 10\,ns$).

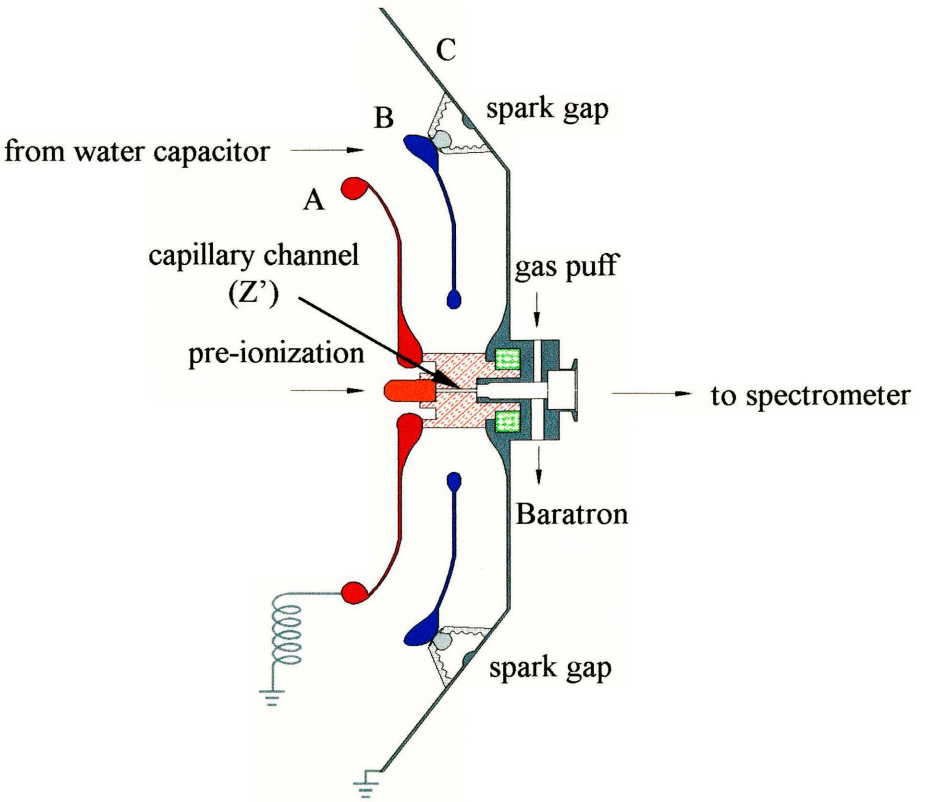

Figure 3.4. Schematic showing a side view cut of the last pulse compression stage, the radial Blumlein transmission line.

This high voltage pulse generator is able to produce peak current pulses of up to 225 kA with 10 ns rise time (10%-90%) and full width half maximum (FWHM) of 20ns over a 1 cm long capillary load. A typical current pulse and the maximum current pulse obtained up to date using this generator, are shown in figure 3.5. The higher amplitude and shorter nature of the pulse shown in the lower part of the figure are the result of a better synchronization of the radial spark-gap switches.

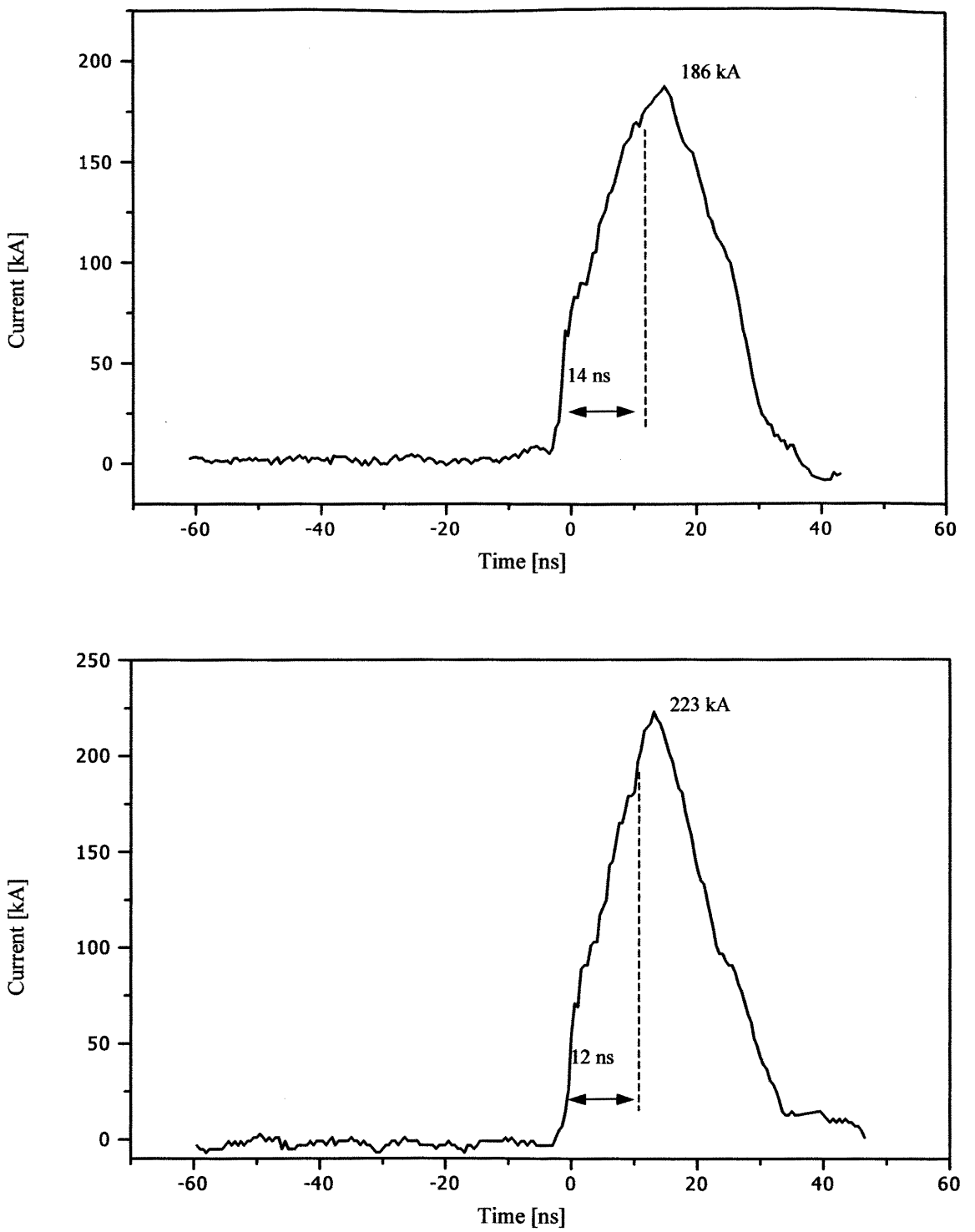

Figure 3.5. Measured current pulses obtained over a 1cm long capillary load. The difference in the amplitude and rise time between the two pulses is due to a better synchronization of the seven spark-gap switches.

In order to obtain a more uniform plasma column suitable for laser amplification, the plasma must be pre-ionized. This is achieved using an auxiliary discharge that generates a low amplitude and slow current pulse. This discharge is triggered 10 μs before the fast current pulse reaches the capillary.

The whole firing sequence involves the synchronization of ten events from the charging of the Marx bank to the time-resolved acquisition of the radiation pulse. The process is entirely controlled by electronics through a computer interfaced console, allowing just one person to drive the entire equipment, including the discharge and the diagnostics.

3.4. Generation of highly ionized plasma column in Argon gas

Time resolved spectroscopy of the plasma columns generated by the experimental setup mentioned in section 3.2. (for a more detailed description see ref. 5) was performed using argon gas. Although argon is not expected to show amplification at wavelengths shorter than 46.9 nm, it was selected because its well known XUV spectral composition and the extensive previous experiments carried out by our group with this gas greatly facilitate its use as a test element to characterize the discharge. The setup used to perform these spectral measurements is schematically shown in figure 3.6. It consists of a gold-coated cylindrical mirror that focuses the radiation emitted by the plasma into the entrance slit of the 2.2 m grazing incidence spectrometer. A fast shutter is placed between the mirror and the spectrometer to protect the optics and the detection elements from the

debris that originates in the electrodes and capillary walls. Inside the spectrometer, a $600\,{}^{l}/_{mm}$ gold-coated diffraction grating place at 4.2° respect to the incoming radiation disperses the different wavelengths along the Rowland circle. Because soft x-ray radiation does not propagate in air, the entire light path is under vacuum $\left(\approx 10^{-5}\,Torr\right)$. The detection system is composed of two micro-channel plates (MCP) arranged in chevron configuration, a phosphorus screen and a charged-coupled device array (CCD). The MCP have a double purpose, they act as intensifier (a gain factor $\sim 10^{5}$) and they provide time resolution by gating the gain for a short time (approximately 5 ns FWHM time resolution). The surface of the MCP exposed to the incoming soft x-ray radiation is coated with MgO to improve the efficiency. The phosphorus screen is used to convert the electrons coming from the MCP to visible light, so then they can be read by the CCD and loaded into the computer for further analysis.

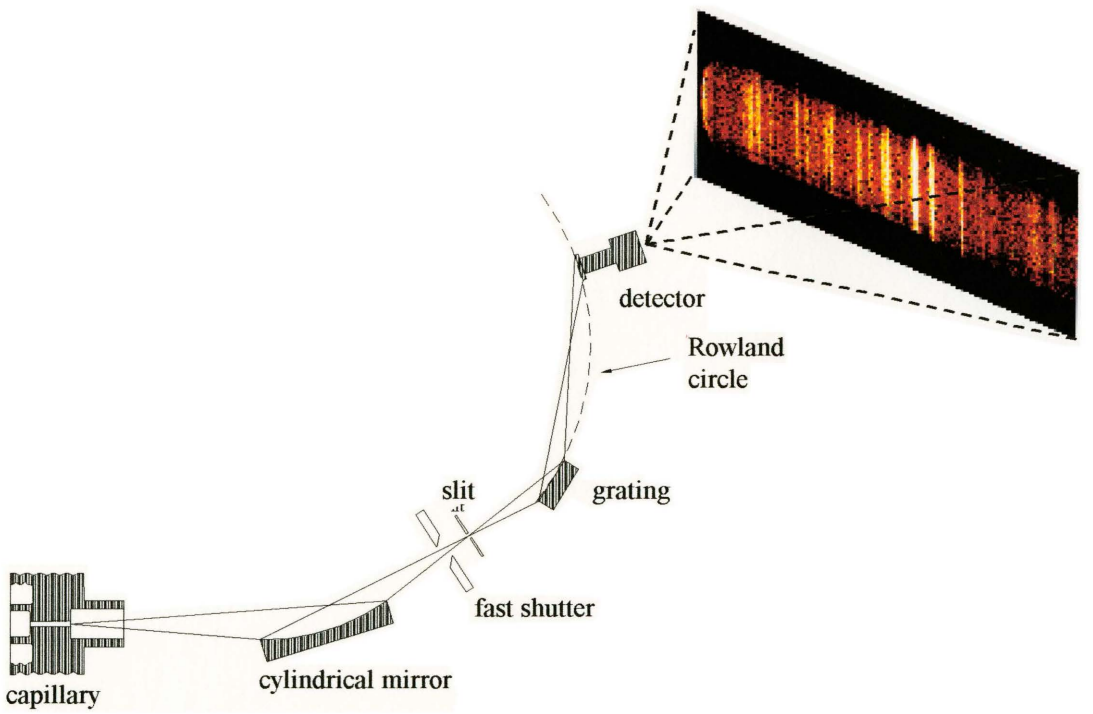

Figure 3.6. Schematic view of the grazing incidence spectrometer used to analyze the radiation emitted by the capillary discharge.

From the observation of the radiation emitted by the different ions present in the plasma for different discharge conditions (current, pressure, and time delay respect to the beginning of the current pulse.), an estimation of the electron temperature can be obtained. Figure 3.7. shows a series of four time-resolved spectra of argon at different times during the plasma compression process with the discharge parameters being approximately the same for all the shots. The data were obtained using a 3 mm diameter by 25 mm long ceramic capillary. The Ar pressure inside the channel was 1 Torr. The time indicated in the upper right corner of each spectrum in figure 3.7 is the delay measured between the beginning of the current pulse and the center of the 5 ns wide detection window. The Ar_{XV} transition appears on the spectrum at 18 ns, but the higher intensity is obtained 25 ns after the start of the current. At this point the plasma is reaching its maximum electron temperature estimated to be around 250 eV. This time will vary accordingly to different discharge conditions like gas pressure, gas composition, capillary diameter, amplitude and rise time of the current pulse, etc.

A similar analysis was done in which the current amplitude was varied. Figure 3.8 compares a series of spectra with a similar time delay. In this case the intensity of the 22.11 nm of Ar_{XV} line increases as the current amplitude increases. What it should be noticed in figures 3.7 and 3.8, more than the intensity of the 22.11 nm transition, is the ratio between this line and the neighboring lines with lower degrees of ionization.

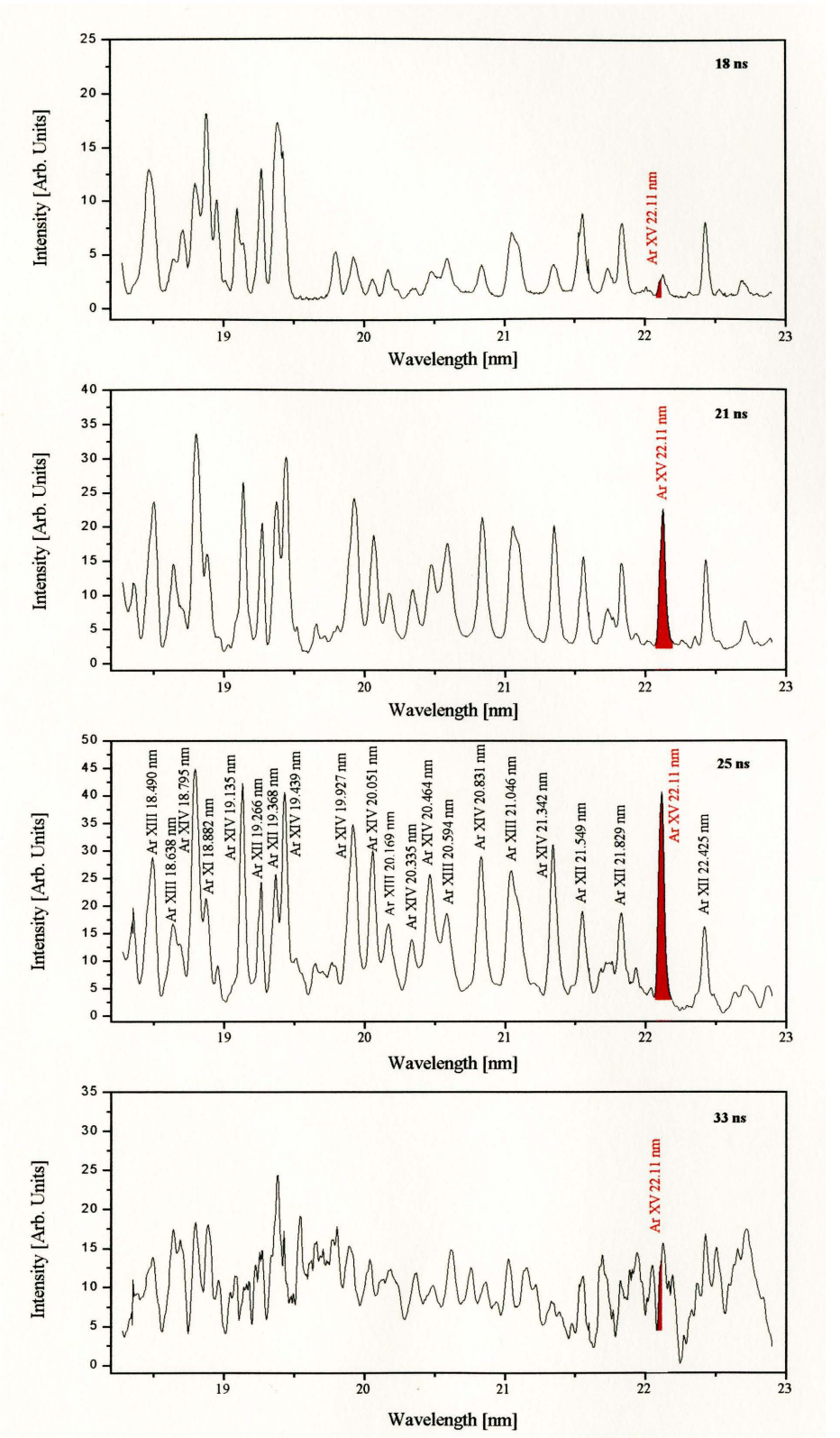

Figure 3.7. Time resolved series of argon spectra for different times respect to the beginning of the current pulse over a 3 mm diameter ceramic capillary. Current magnitude 195 kA and Ar pressure 1 Torr.

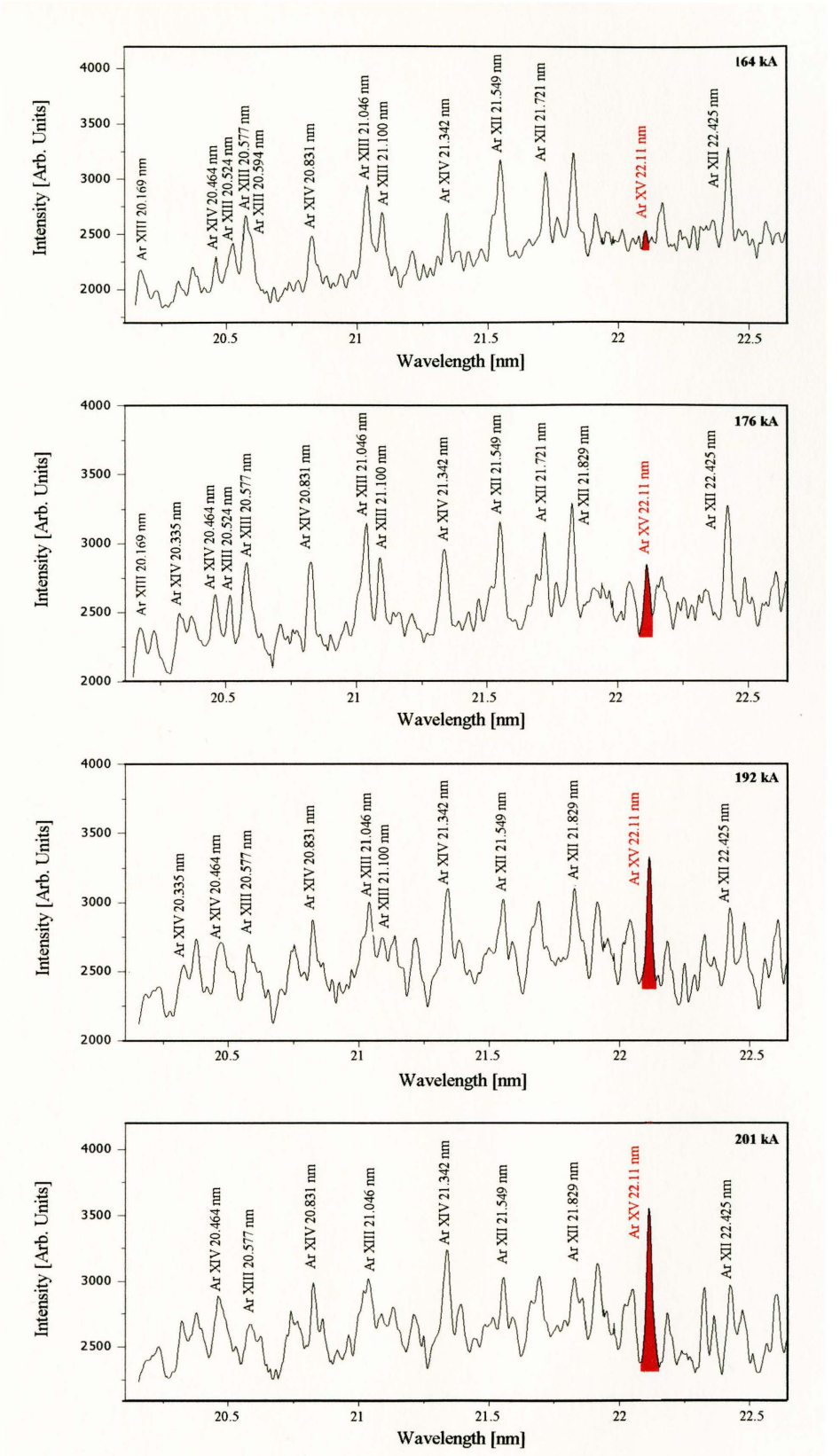

Figure 3.8. Time-resolved series of argon spectra for different current pulse values over a 3 mm diameter ceramic capillary with a gas pressure of 1Torr.

3.5. Effect of heavy atoms

It is well known in plasma physics that the presence of heavy elements in plasmas can contribute to significantly cool the plasma through intense line radiation, that constitute important losses in the energy balance equation. In order to verify the feasibility of the generation of highly ionized species in heavier elements, a useful study is to observe the spectrum of the radiation emitted by a particular ion when a heavier element is added to the plasma.

In the experiment discussed in this section, time resolved spectroscopy of an Ar-Xe gas mixture was performed for different proportions of xenon gas. Figure 3.9 shows a series of spectra in the 20-23 nm region for different mixing proportions.

The mixture of the gases was realized inside a separated container equipped with a rotary vane and a pressure gauge. The desired mixture proportions are achieved adjusting the partial pressure of the gases. The gases are agitated for about 15 min before the mixture is injected into the capillary.

From figure 3.9 it can be seen that, even with 20 % of xenon gas in the mixture, the argon line at 22.11 nm corresponding to Ar_{XV} is still present in the spectrum. This result gives some confidence in trying to obtain higher degree of ionization in heavier elements. In order to study cadmium as a heavy element medium for lasing at shorter wavelenths, a room temperature metal vapor source was developed to produce and inject vaporized cadmium into the capillary channel. The next section discusses this cadmium source in some detail.

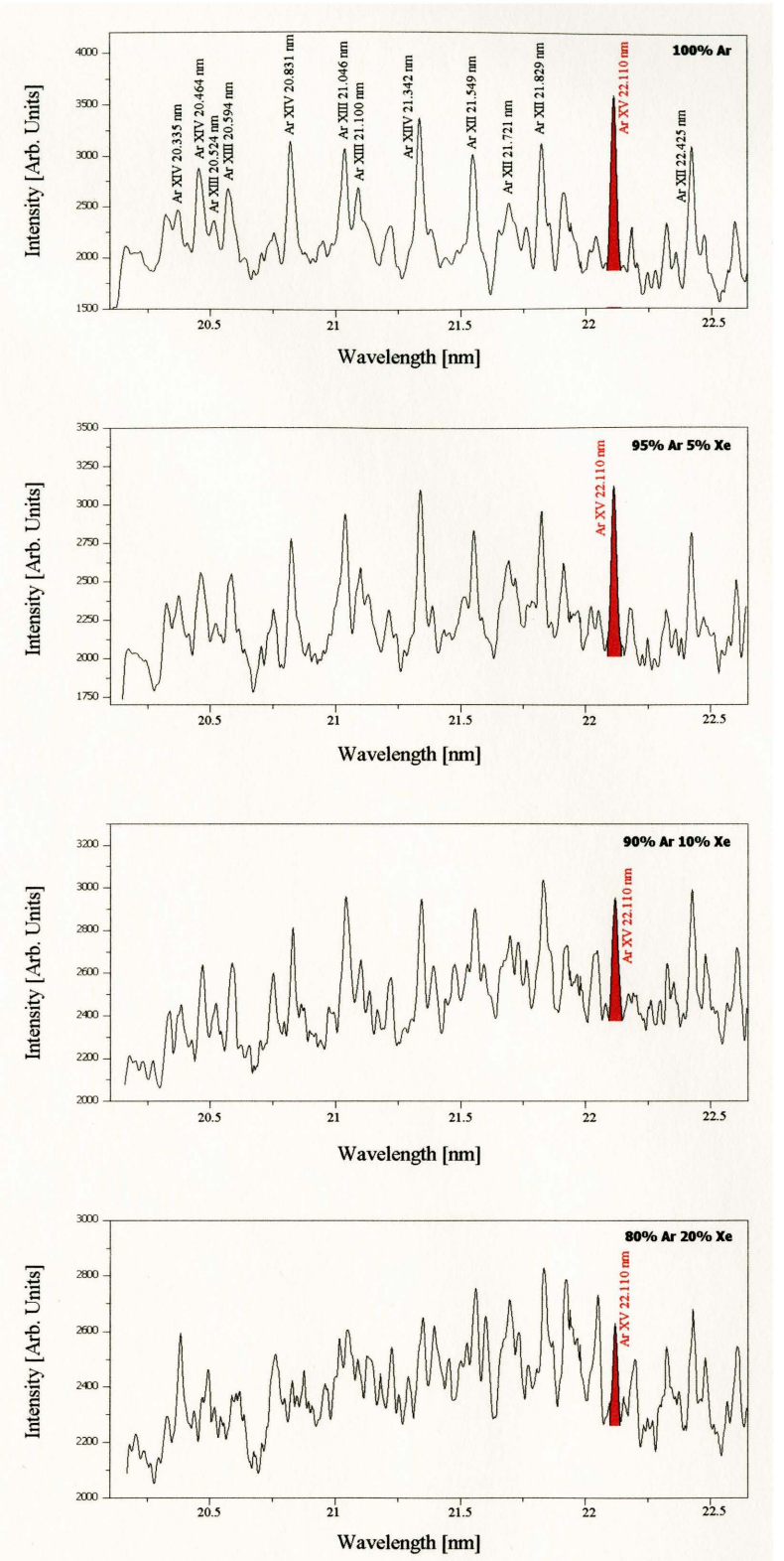

Figure 3.9 Series of four spectra with same discharge conditions and different gas composition, ranging from pure argon to 80 % argon and 20 % xenon. Delrin capillary 4 mm in diameter, 195 kA, and 1T.

3.6. Development of room temperature metal vapor source.

Like most metals at room temperature, cadmium, is found in the solid state. In order to uniformly fill the capillary channel with cadmium vapor, the metal first needs to be vaporized. Although the simplest way to create vapor out of a metal is by heating up a small sample of the material, an alternative technique had to be developed because the geometry of the discharge makes impossible the implementation of an oven in the region where the high voltage is present. In order to create a reasonable uniform metal vapor column inside the capillary channel, a small discharge that uses a cadmium electrode was designed. Figure 3.10 illustrates the implementation of this discharge in the setup shown in figure 3.4. A scheme of the pulse generator is also shown.

A discharge between the cadmium electrode and the ground electrode produces a current pulse that can be varied from 1.5 kA to 15 kA in order to create different cadmium densities inside the capillary channel. This controlled current pulse is triggered $10\,\mu s$ before the pre-ionization discharge is fired in the capillary, creating a metal vapor jet that completely fills the capillary channel.

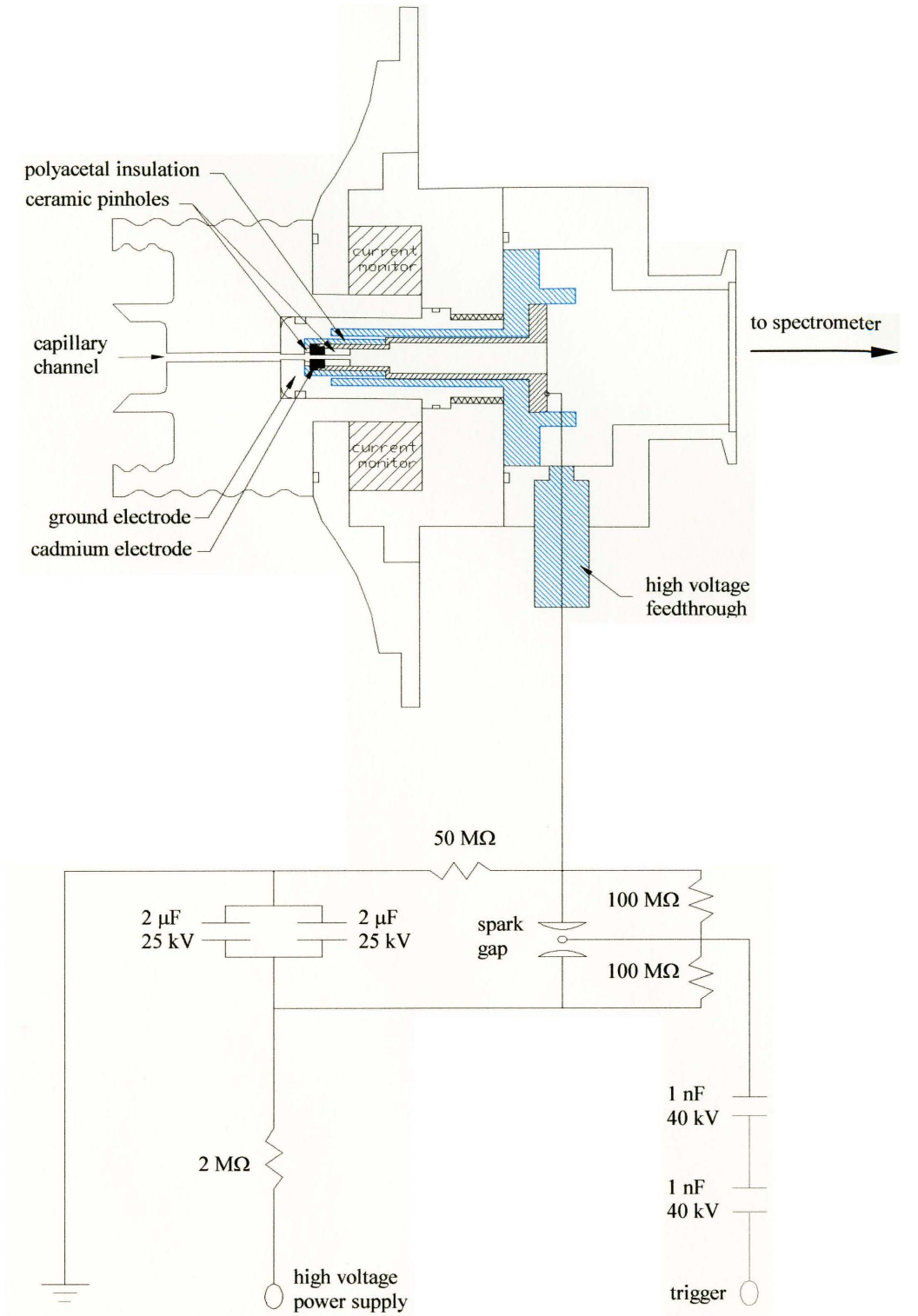

Figure 3.10. Schematic diagram of the room temperature metal vapor source and the corresponding pulse generator

In order to achieve a significant gain-length product, the plasma column created must be uniform over a certain length, it must have the right temperature and density and it must be very pure in cadmium composition. With the purpose of determining the purity of the metal vapor generated by the small discharge setup, spectral measurements of the cadmium vapor were taken using a visible normal-incidence spectrometer with a 300 l/mm grating. From figure 3.11. it can be seen that no significant spectral lines other than cadmium transitions were observed over a wide range of wavelengths from ultraviolet to the infrared end of the visible region of the spectrum.

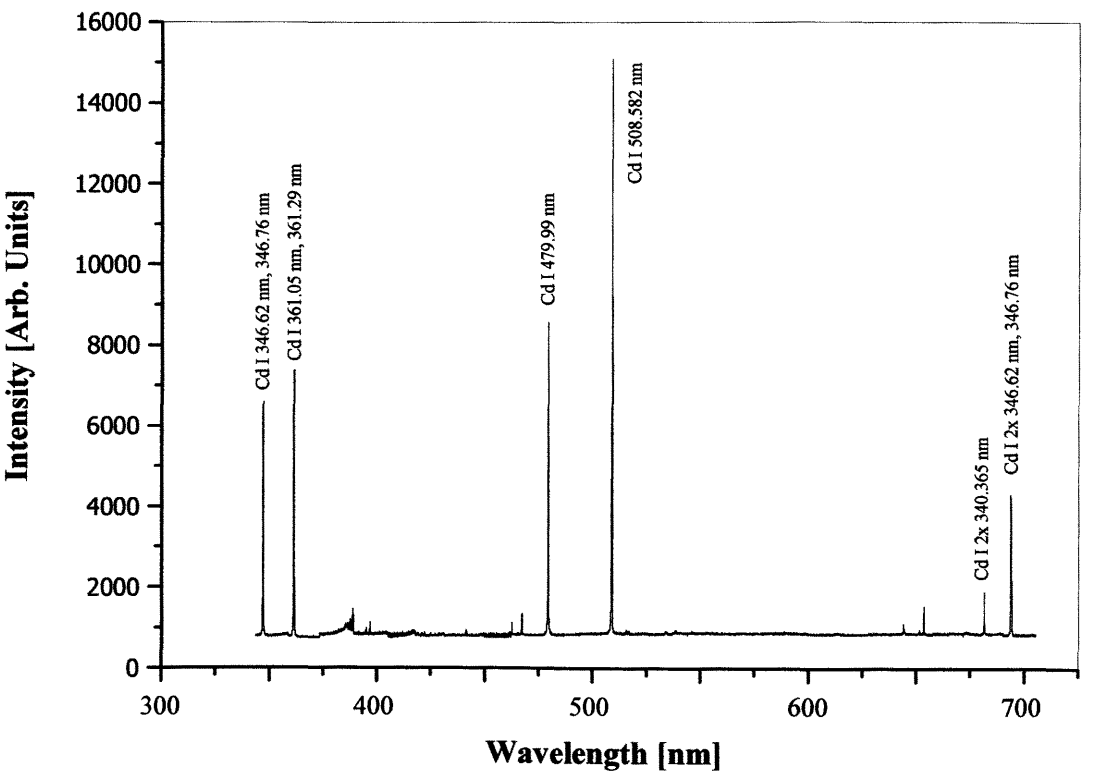

Figure 3.11. Spectrum in the visible region of the cadmium vapor generated by the setup shown in figure 3.10.

The fact that in the spectrum shown in figure 3.11 only the cadmium transitions are visible, is a clear indication that the composition of the vapor created is practically atomically pure cadmium.

In the next section the first results corresponding to the generation of highly ionized Cd plasma column using a capillary discharge are discussed.

3.7. Experimental results

In order to determine the degree of ionization obtained in a capillary discharge created cadmium plasma, several spectra at very different discharge conditions were taken. In a first series of observation, the region covering from 23 nm to 26 nm, was studied using a 600 l/mm grating. This spectral region is of particular interest because it contains a large number of Cd_{XXI} transitions, the specie of interest for the generation of soft x-ray amplification. Also lines of Cu-like Cd are present in this region[6,7,8,9,10,11]. Figure 3.12. shows a time resolved spectrum, corresponding to a polyacetal capillary 4 mm in diameter, as observed with a CCD after conversion from soft x-ray to visible radiation is achieved by mean of the MCP-phosphorus combination previously described. This image can be vertically integrated to give origin to the spectrum shown in figure 3.13.

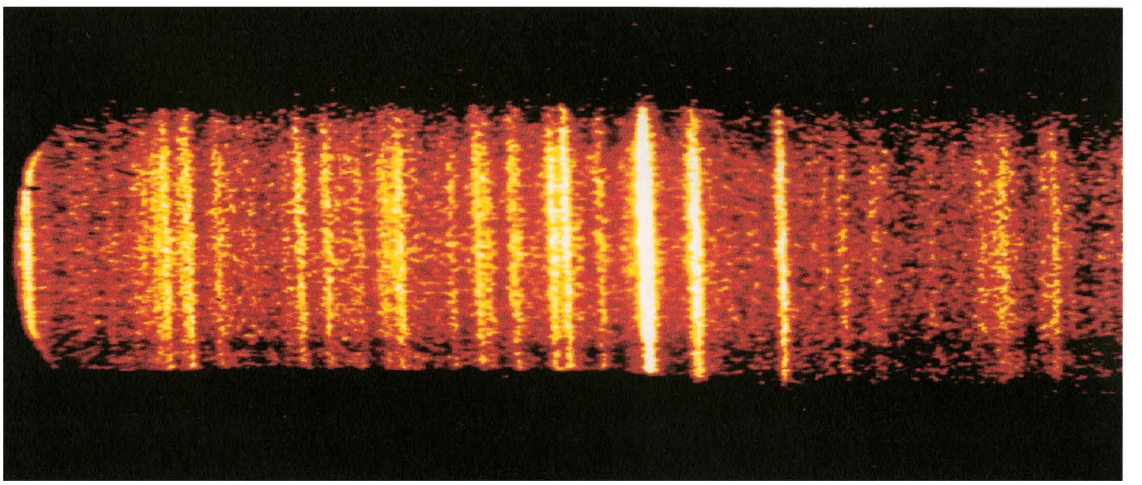

Figure 3.12. 2-D image obtained directly from the CCD corresponding to a cadmium spectrum in the 23-26 nm spectral region.

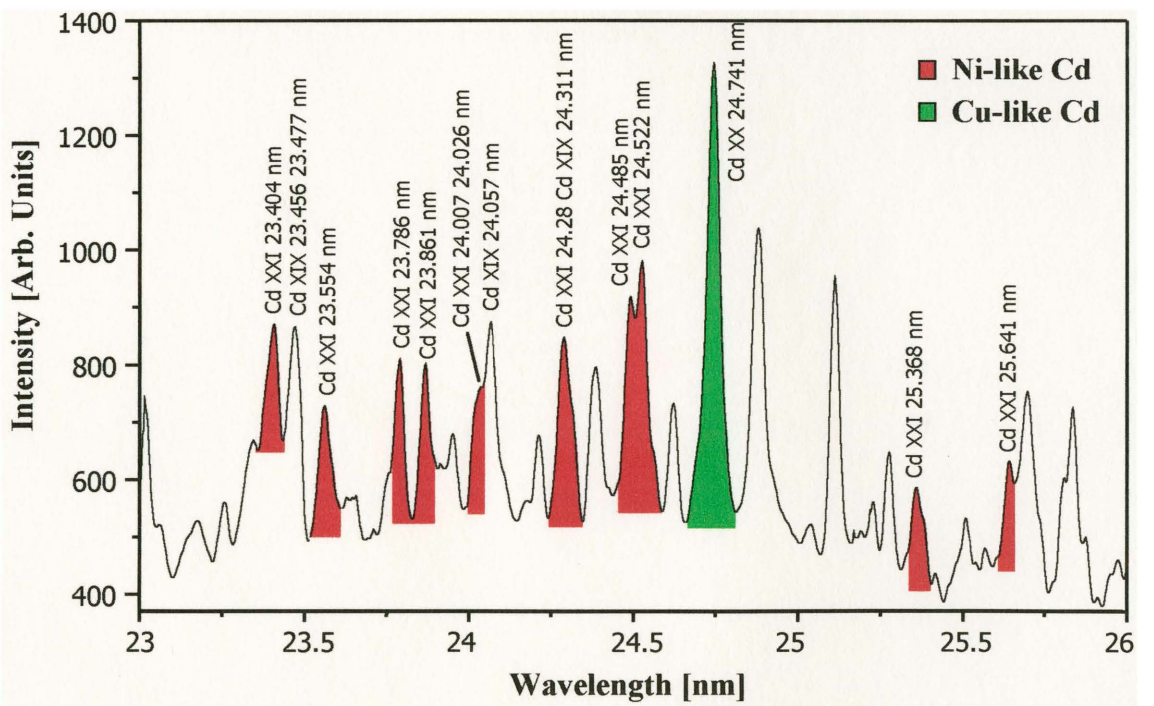

Figure 3.13. Vertically integrated version of spectrum shown in fig. 3.11. The cadmium plasma column was generated by a 175 kA current pulse and spectrum was recorded 30 ns after the beginning of the current pulse.

The observation of a radiative transition from a higher energy level to the laser upper level can also be considered a good indicator in the creation of a more favorable plasma condition for the occurrence of the laser emission. For that purpose two transitions were studied, the 18.0218 nm and the 18.0299 nm corresponding to Cd XXI[10,12]. Since these two lines are only 0.0081 Å apart, a 2400 l/mm grating had to be used in order to achieve enough resolution to differentiate the two transitions. Figure 3.14 is a spatially integrated spectrum of that region.

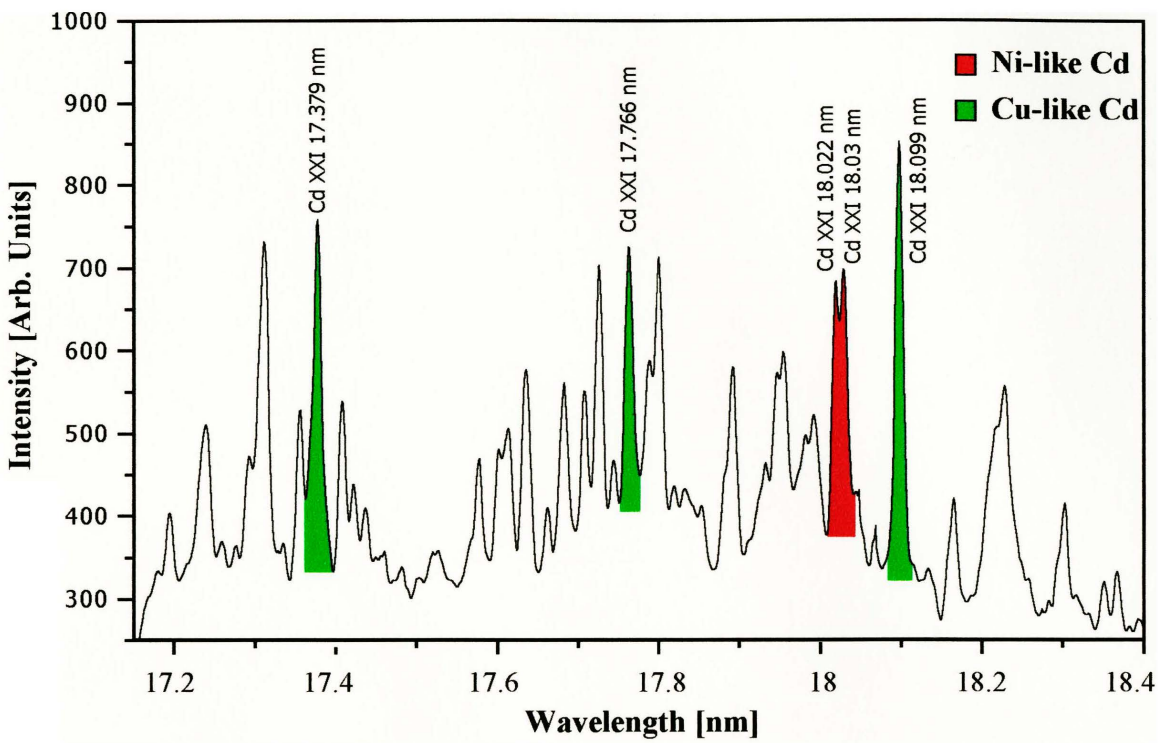

Figure 3.14. Vertically integrated spectrum around the 18.0 nm region. A 2.2 m grazing incidence spectrometer with a 2400 l/mm grating was used. The cadmium plasma was excited by a 180kA current pulse and spectrum was recorded 35 ns after the beginning of the current pulse.

From the argon data, an increment in the degree of ionization was observed when a capillary with a ceramic channel was used instead of the most common polyacetal channel. This can be explained by the fact that in the capillary with ceramic channel less material is ablated from the walls by the fast current pulse, resulting in a hotter plasma.

For the case of the cadmium plasma the data evidenced the opposite behavior, and proof of this can be seen in figure 3.15. These spectra correspond to a two different capillary material with the same discharge conditions. Figure 3.15 (a), that covers the 23-26 nm spectral region, compares the behavior of several $4p-4s$ transitions in Ni-like Cd. Figure 3.15 (b) shows a similar comparison in the 17.2-18.4 nm region, where two Ni-like Cd $4d-4p$ transitions are observed in the vicinity of 18 nm. One possible explanation is that after a few discharge shots, a metal coating develops inside the channel, turning the inner wall of the capillary into a conductor. When the current pulse reaches the load in the next shot, most of the current starts flowing through the wall thereby producing a much cooler and less dense plasma. When a polyacetal capillary is used, the material ablated from the walls in each shot helps to prevent the formation of the metallic coating, obtaining a better degree of ionization.

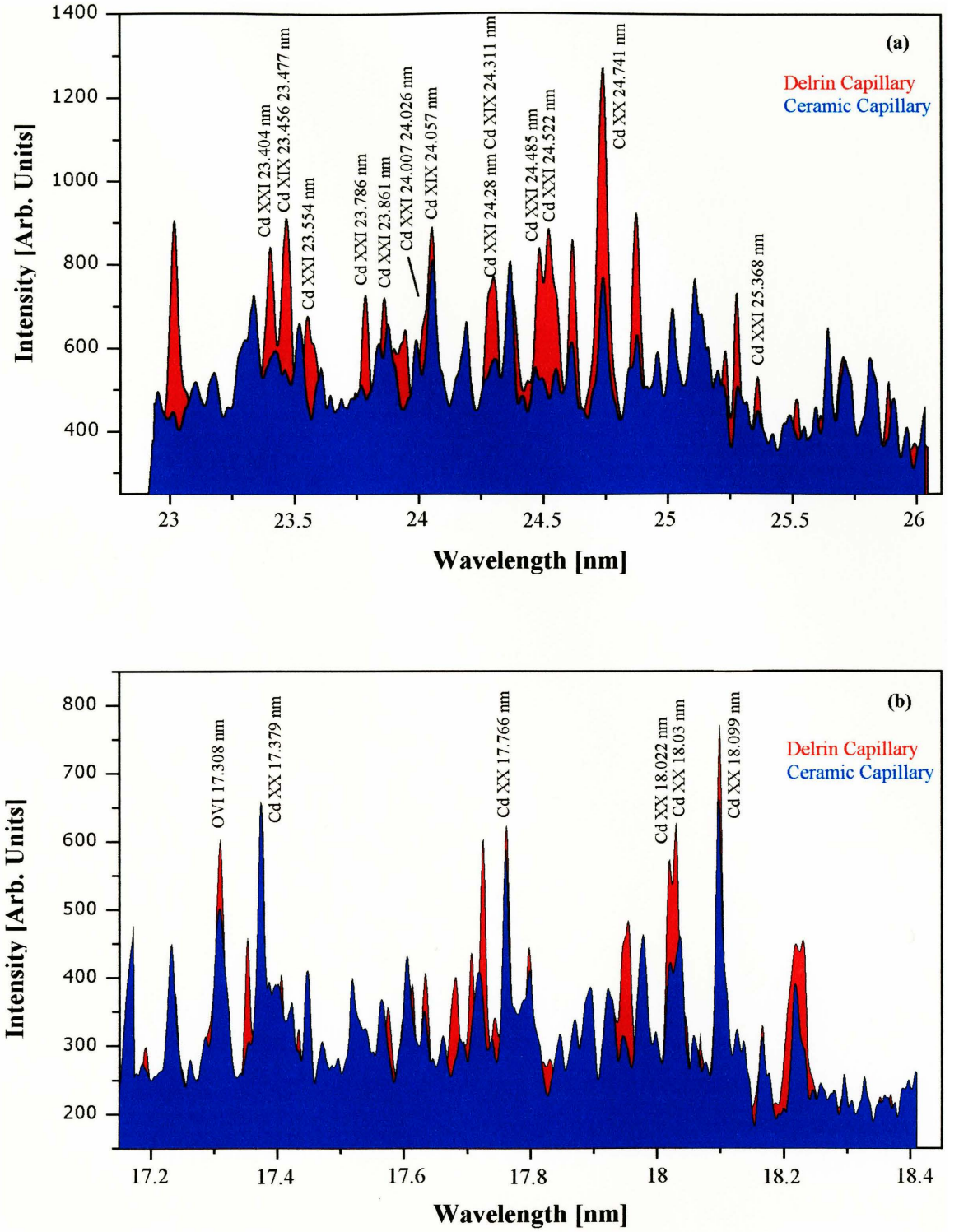

Figure 3.15. Comparison between delrin and ceramic capillary channels for: (a) the 4p-4s transitions and (b) the 4d-4p transitions. All spectra were taken over 4 mm in diameter and 20 mm in length capillaries at 175 kA current pulse, and 35 ns after the beginning of the current pulse.

In order to understand the behavior of the cadmium plasma column, several shots were fired varying different discharge parameters like discharge current, observation time, and current in the metal vapor source that controls the cadmium vapor density. Shots with the same fixed parameters were grouped forming series for a more clear comparison.

The first discharge parameter changed was the magnitude of the excitation current in a delrin capillary, ranging from 100 kA, where the Cd_{XXI} transitions are just appearing, to 190 kA where the Ni-like cadmium lines are among the most intense lines on the spectra as it can be seen in figure 3.16.

Another relevant parameter to be analyzed is the time elapsed between the beginning of the current pulse and the time when the spectrum is recorded. The acquisition of the radiation takes place during a narrow time window, allowing for time resolution analysis to be performed on each spectrum. This type of study provides the moment in time when the maximum ionization occurs, based on the behavior of the ratio between the Cd_{XXI} and Cd_{XX} lines. This time depends on many factors such as the diameter and the composition of the capillary channel, the type and pressure of the gas injected, etc. A typical temporal series for a 5 mm diameter delrin capillary is presented in figure 3.17. Maximum intensity of the Ni-like Cd lines is observed at a time delay of 37 ns respect to the beginning of the current pulse.

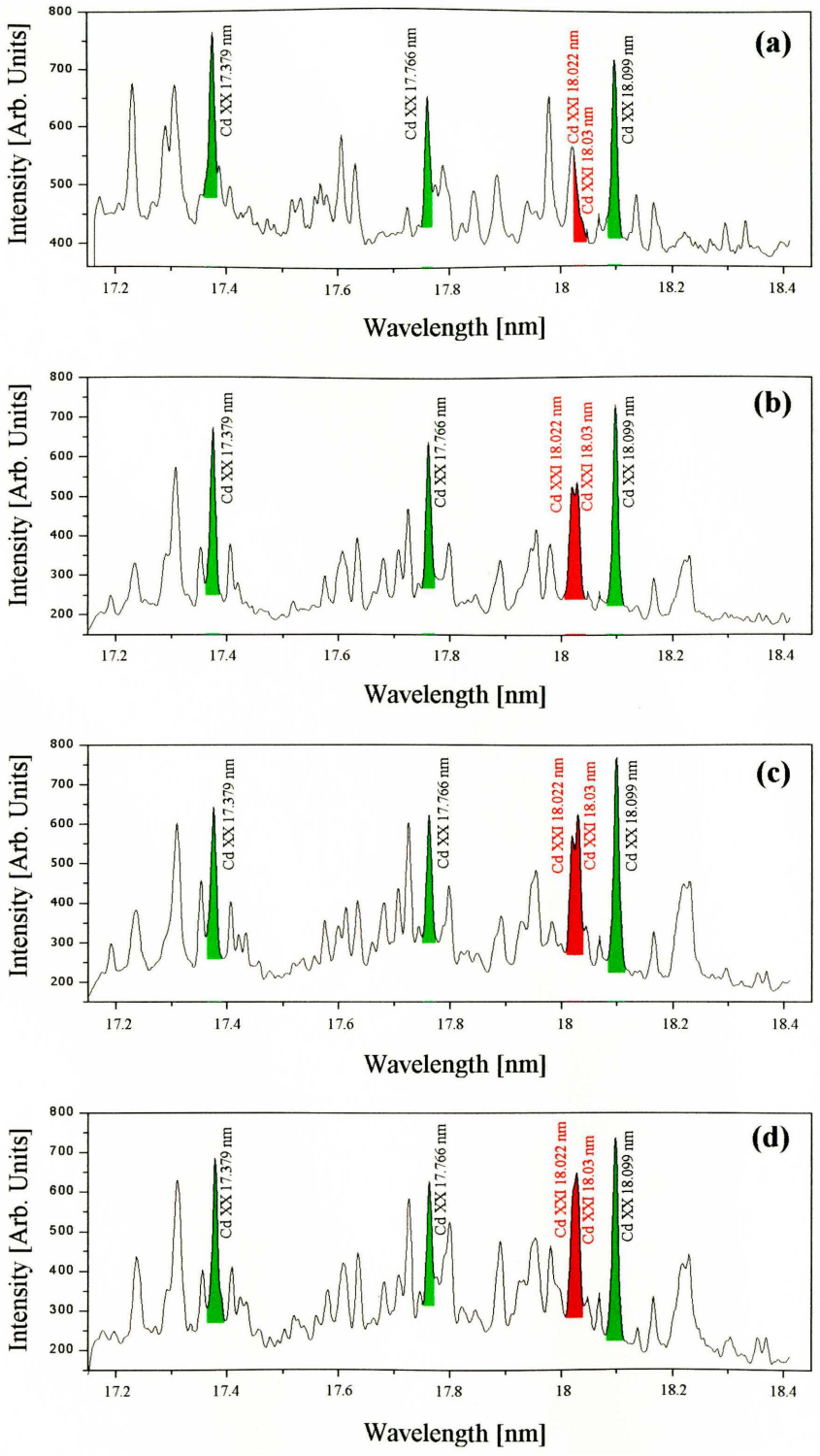

Figure 3.16. Series of cadmium spectra showing the correlation between the intensity of the Ni-like cadmium transitions and the magnitude of excitation current pulse. All four spectra were recorded 37 ns after the beginning of the current pulse under the same cadmium vapor pressure. (a) 103 kA. (b) 132 kA. (c) 171 kA. (d) 192 kA.

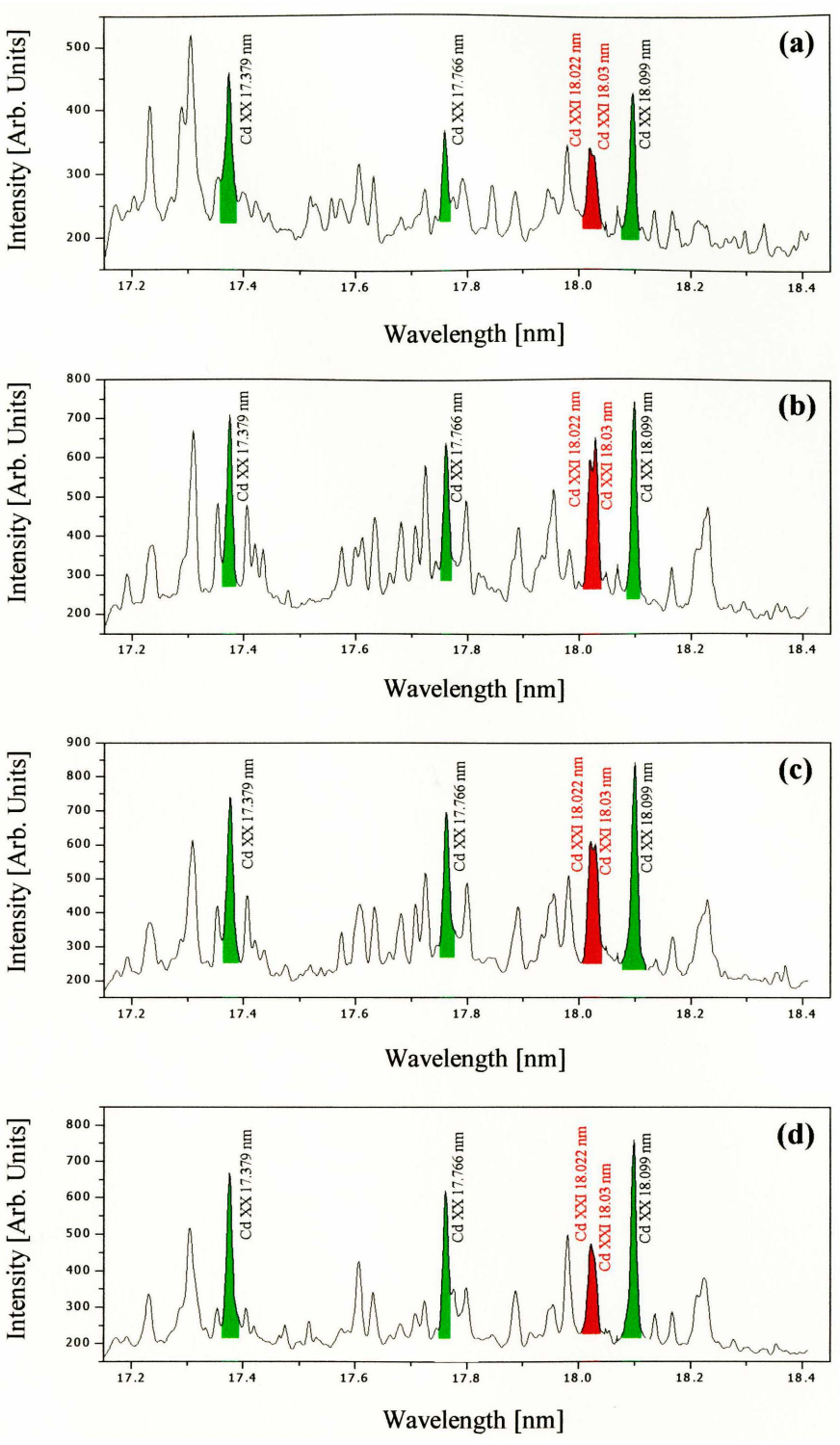

Figure 3.17. Temporal series of cadmium spectra corresponding to a 5 mm diameter, 20 mm in length delrin capillary. All four spectra were taken under the same discharge conditions, 170 kA current pulse and 4.2 kA of cadmium pre-discharge to ensure the same cadmium density over all the series. (a) 29 ns, (b) 37 ns, (c) 44 ns, (d) 52 ns from the beginning of the current pulse.

An additional parameter over which we have control is the cadmium density inside the capillary channel at the moment of the current pulse. This density is controlled by the current magnitude of the pre-discharge in the cadmium electrode. In figure 3.18 a series of spectra can be seen as the cadmium density is changed varying the pre-discharge current. The intensity of the Cd_{XXI} lines is observed to increase as a function of the Cd discharge current up to ~4.5 kA, after which the degree of ionization is observed to decrease, probably due to a reduction in the electron temperature caused by the higher Cd vapor densities. Although more current through the cadmium electrode represents more metal vapor generated, a characterization of the cadmium density as a function of the pre-discharge current still needs to be completed.

The last degree of freedom that we can adjust to try to create a highly ionized plasma is the length and diameter of the capillary channel. While the length of the channel should not greatly affect the plasma parameters if the rest of the discharge conditions are maintained constant, the diameter is closely related to the electron temperature and density of the plasma at the moment of the pinch. In figure 3.19 a comparison between two spectra corresponding to a 4 mm and 5 mm channel diameter is presented. Both spectra were taken under the same discharge conditions on a delrin capillary.

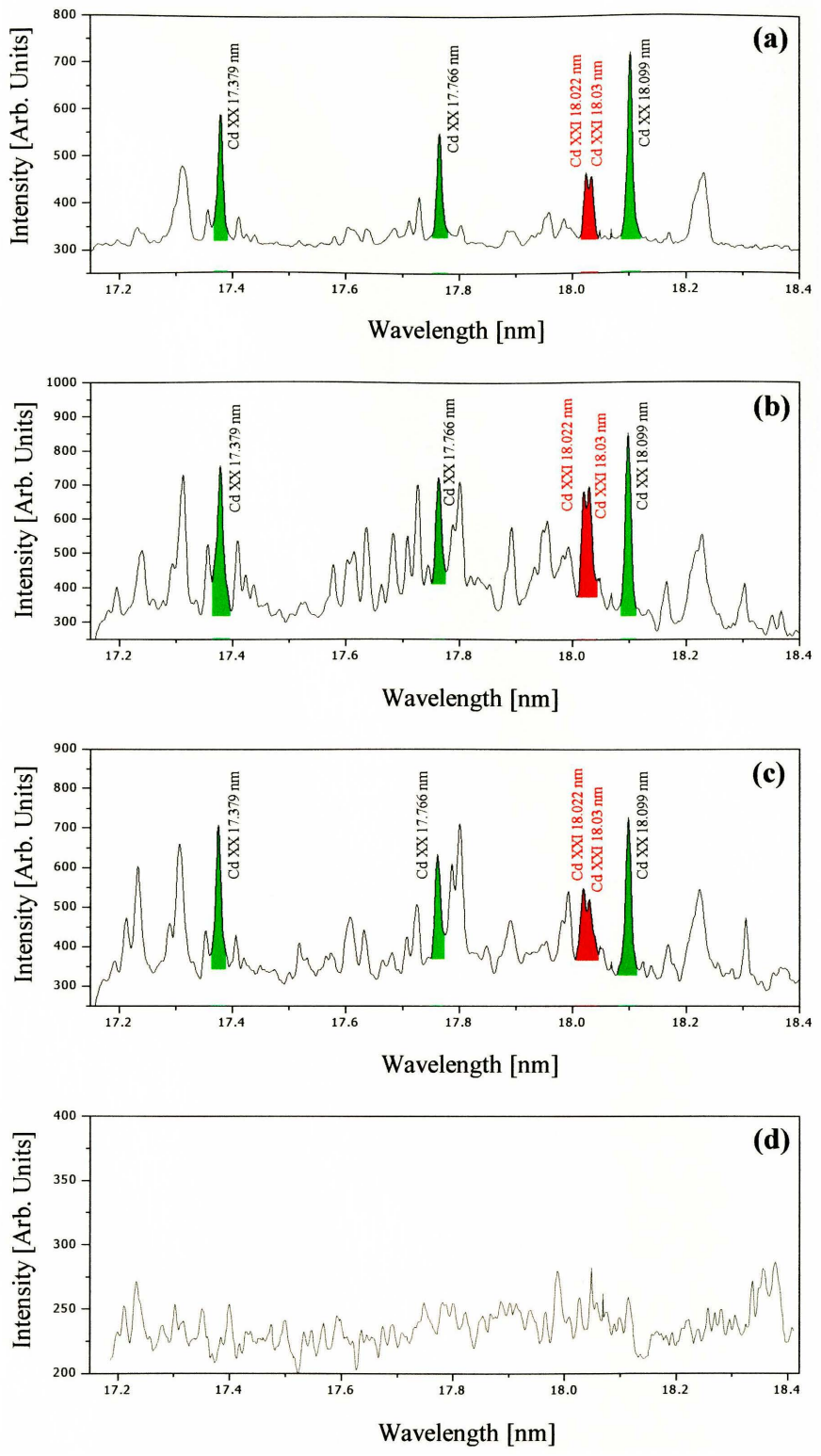

Figure 3.18. Series of cadmium spectra showing the correspondence between the relative intensity of the Cd XXI lines vs. the cadmium density for a 5 mm delrin capillary. All four spectra were taken under the same discharge conditions, 180 kA at 37 ns after the beginning of the current pulse. (a) 2 kA, (b) 4.6 kA, (c) 5.9 kA, (d) 7.25 kA current in the cadmium electrode.

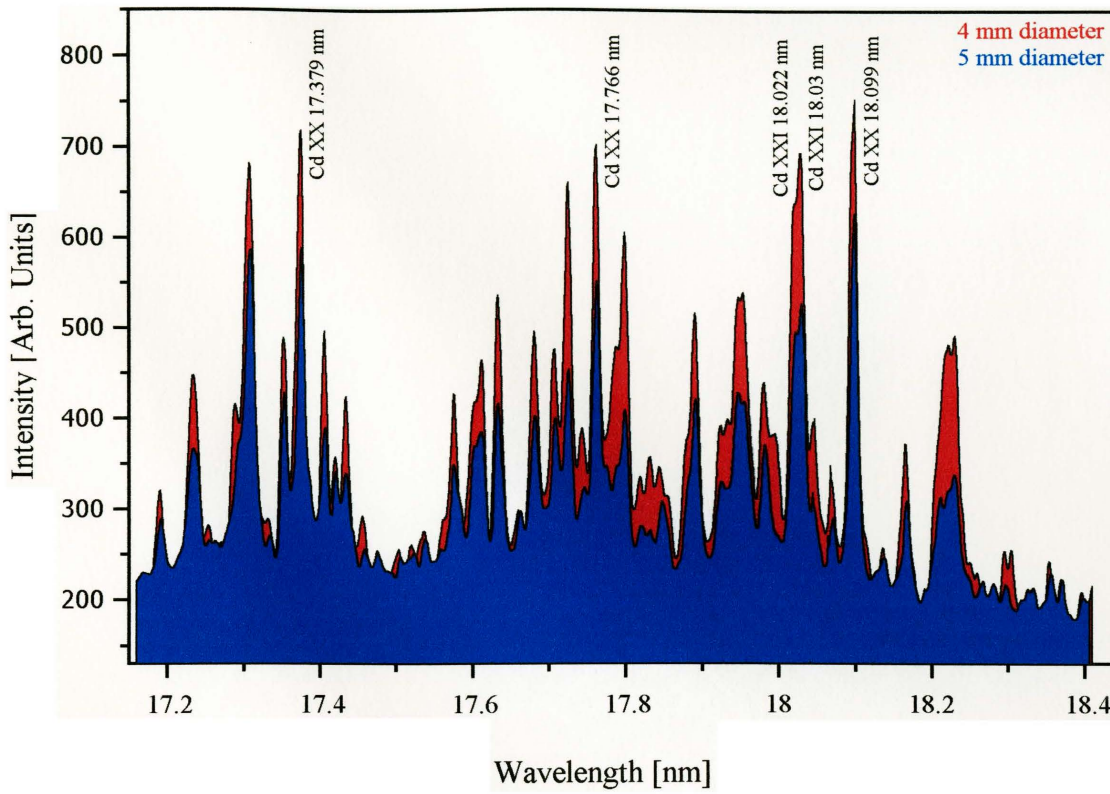

Figure 3.19. Comparison between two cadmium spectra corresponding to capillary channels 4 mm and 5 mm in diameter and 20 mm in length. In both cases, the discharge current was 175 kA, the time elapsed from the beginning of the current pulse was 32 ns and the pre-discharge current in the cadmium electrode was 4 kA.

While moving towards smaller diameter channels seems to improve the ionization degree, in practice, there is a difficulty that still has to be addressed. This is the large mechanical stress imposed to the capillary structure when the current pulse reaches the load. In experiments conducted for this purpose, the lifetime of the capillaries was observed to decrease from hundred shots to about forty shots when the diameter was reduced from 5 mm to 4 mm in delrin capillaries. The lifetime decreased to less than ten shots for capillaries with 3 mm channels. Similar degradation was observed when the length of the capillary channel was increased from 20 to 35 mm.

In summary, the generation of Ni-like Cd in a capillary discharge has been demonstrated. This result constitutes a first encouraging step towerds the demonstration of a discharge-pumped Ni-like Cd laser. As discussed in chapter 4 of this thesis, additional work needs to be completed before laser amplification can be observed in this ion.

3.8. References

[1] A. N. Zherikhin, et al. Sov. J. Quant. Electron. 6, 82 (1976); A. V. Vinogradov and V. N. Shlyaptsev, Sov. J. Quant. Electron. 13, 303 and 1511 (1983), and references therein.

[2] S. Maxon, P. Hagelstein, B. MacGowan, R. London, M. Rosen, J. Scofield, S. Halhed, and M. Chen, Phys. Rev. A 37 2227 (1988); also, W. H. Goldstein, J. Oreg, A. Zigler, A. Barshalom, and M. Klapisch, Phys. Rev. A 38 1797 (1988).

[3] J.J. Rocca, V. N. Shlyaptsev, F. G. Tomasel, O. D. Cortazar, D. Hartshorn and J. L. A. Chilla, "Demonstration of a Discharge Pumped Table-Top Soft-X-Ray Laser", *Phys. Rev. Lett.* **73**, pp. 2192-2195, 1994.

[4] S. M. Zakarov, A. A. Kolomenskii, S. A. Pikuz and A. I. Samokhin, *Pis'ma Zh. Tekh. Fiz.* **6**, pp. 1135, 1980. [*Sov. Tech. Phys. Lett.* **6**, pp. 486, 1980].

[5] J. J. Gonzalez, M. Frati, J. J. Rocca and V. N. Shlyaptsev, "First experimental results of a very high power density capillary discharge plasma", Proc. Of the X-ray Lasers Conf., pp. 163-166, 1998.

[6] J. Sugar, V. Kaufman, D. H. Baik, Y. K. Kim, and W. L. Rowan, J. Opt. Soc. Am. B 8(9), 1795-8 (1991).

[7] U. Litzén, and X. Zeng, J. Phys. B: At. Mol. Phys. 24, L45-L50 (1991).

[8] N. Acquista, and J. Reader, J. Opt. Soc. Am. B 4(1), 649-51 (1984).

[9] S. S. Churilov, A. N. Ryabtsev, and J. F. Wyart, Physica Scripta 38, 326-35 (1988).

[10] U. Litzén, and X. Zeng, Physica Scripta 43, 262-5 (1991).

[11] J. Reader, N. Acquista, and D. Cooper, J. Opt. Soc. Am. 73(12), 1765-70 (1983).

CHAPTER IV

4.1. Summary

The work conducted in this thesis was motivated by the possibility of demonstrating the generation of soft x-ray and extreme ultraviolet coherent radiation by capillary discharge excitation at new wavelengths.

The generation of $10\,\mu J$ laser pulses at 52.9 nm was demonstrated and characterized utilizing a very compact capillary discharge. This new 23.4 eV tabletop laser is of particular interest as a high energy photon source for photochemistry and photophysics studies in which He is used as a carrier or buffer gas. This result extends the number of laser transitions available from high intensity tabletop capillary discharge excited lasers. In addition to this one, are the previously reported laser transitions using the same pumping scheme, the $3p\,^1S_0$ - $3s\,^1P_1$ in Ne-like Ar at 46.9 nm and Ne-like S at 60.8 nm.

The second part of this thesis presented a new source capable of inserting metal vapor produced at room temperature into the capillary channel. Spectroscopy over the entire visible region of the cadmium vapor generated with this source was realized in order to determine the purity of the resulting gas produced and spectra where only

cadmium transitions could be seen were obtained, proving evidence that the device is able of generating atomically pure Cd vapor .

In addition, the utilization of a very powerful capillary discharge, in conjunction with the metal vapor source, leaded to the observation of Ni-like Cd (Cd^{+20}) transitions. Extensive studies were performed over the plasma by changing different parameters of the discharge such as current magnitude, time of observation, gas density, capillary channel size and composition, etc.

Although the observation of strong radiation in the Ni-like Cd transitions represents an encouraging step, much more needs to be done before the demonstration of amplification at 13.2 nm is achieved. Part of future work should include the study of the homogeneity and stability of the plasma column utilizing a time-resolved pinhole camera. A direct measurement of the cadmium density and electron density that characterize the plasma column will be necessary to optimize the conditions for lasing. After these steps are completed it will be possible to begin the search for laser action in the 13.2 nm Ni-like Cd transition. Since the experiment involves many parameters, the search for gain must be done systematically and in coordination with model calculations.